Biomaterials. Author manuscript; available in PMC 2022 December 10.

Published in final edited form as:
Biomaterials. 2022 February 01; 281: 121363. doi:10.1016/j.biomaterials.2022.121363.

Differential bioactivity of four BMP-family members as function of biomaterial stiffness

Adrià Sales[1,2,#], **Valia Khodr**[1,2,*], **Paul Machillot**[1,2,*], **Line Chaar**[3], **Laure Fourel**[1,2,3], **Amaris Guevara-Garcia**[1,2,3], **Elisa Migliorini**[1,2], **Corinne Albigès-Rizo**[3], **Catherine Picart**[1,2,4,#]

[1]Interdisciplinary Research Institute of Grenoble (IRIG), ERL BRM 5000 (CNRS/UGA/CEA), CEA Grenoble, 17 rue des Martyrs, 38054 Grenoble cedex, France

[2]CNRS, Grenoble Institute of Technology, LMGP, UMR 5628, 3 Parvis Louis Néel, 38016 Grenoble

[3]INSERM U1209, CNRS 5309, Université de Grenoble Alpes, Institut for Advanced Biosciences, Institut Albert Bonniot, Allée des Alpes, Site Santé, 38700 La Tronche, France

[4]Institut Universitaire de France (IUF)

Abstract

While a soft film itself is not able to induce cell spreading, BMP-2 presented via such soft film (so called “matrix-bound BMP-2” was previously shown to trigger cell spreading, migration and downstream BMP-2 signaling. Here, we used thin films of controlled stiffness presenting matrix-bound BMPs to study the effect of four BMP members (BMP-2, 4, 7, 9) on cell adhesion and differentiation of skeletal progenitors. We performed automated high content screening of cellular responses, including cell number, cell spreading area, SMAD phosphorylation and alkaline phosphatase activity. We revealed that the cell response to bBMPs is BMP-type specific and involved certain BMP receptors and beta chain integrins. In addition, this response is stiffness-dependent for several receptors. The basolateral presentation of the BMPs allowed us to discriminate the specificity of cellular response and the role of type I and II BMP receptors and of β integrins in a BMP-type and stiffness-dependent manner. Notably, the role of BMP-2 and BMP-4 were found to have distinct roles, while ALK5, previously known as a TGF-β receptor was revealed to be involved in the BMP-pathway.

Keywords

biomimetic films; stiffness; adhesion; differentiation; BMPs; integrins

[#]co-corresponding authors: Adrià Sales, Catherine Picart adria.sales88@gmail.com; catherine.picart@cea.fr.
[*]Co-second authors

Author contribution

C.P. supervised the project, designed the experiments, wrote the manuscript, acquired funding and provided the resources. A.S and P.M. designed, and performed experiments, analyzed the data, and wrote the manuscript. V.K. carried out experiments, analyzed the data and edited the manuscript. L.F. and C.A.R provided advice and technical assistance, and edited the manuscript. E.M. and A.G.G reviewed and edited the manuscript.

Competing interests

The authors declare that they have no conflict of interest with the contents of this article.

Europe PMC Funders Author Manuscripts

Europe PMC Funders Author Manuscripts

1 Introduction

Bone morphogenetic proteins (BMPs) belong to the transforming growth factor β superfamily [1] and are known to participate in a large number of physiological and pathological processes, including cell growth and differentiation [2], tissue development [3], as well as cancerous processes [4,5]. BMP signaling, which is mediated via BMP type I and type II receptors, involves different pathways usually described as SMAD or non-SMAD, and is dependent on the mechanical context of the cell environment [6]. BMP signaling pathway is under the control of multiple ligands binding two type I and two type II receptors that interact combinatorically to form distinct receptor-ligand complexes [7]. In addition, the repertoire of BMP ligands and of BMP receptors is cell- and tissue-dependent context [8].

BMPs can either be diffusible molecules or be presented by extracellular matrix (ECM) components [9]. It is known that BMP-mediated signaling depends on the duration of exposure to BMPs and on their spatial localization [10,11]. A sustained presentation of the BMP ligands can be obtained using biomaterials such as a collagen [12], a poly(ethyl acrylate) polymer [13], or a polyelectrolyte film containing hyaluronic acid and poly(L-lysine) [14].

Beside their role in cell differentiation, BMPs appear to induce cell spreading and they also appear to control cytoskeleton organization and cell migration [15,16]. Increasing evidences highlight a role of BMPs in mechanotransduction [6,17,18]. Mechanotransduction via the ECM is known to involve the adhesion receptors integrins and to be sensitive to matrix stiffness [19,20]. Indeed, BMP signaling can be modulated by integrins [21], matrix stiffness and cytoskeletal tension [22].

We have previously shown that a biomimetic material presenting BMP-2 in a matrix-bound manner (bBMP-2) can be used to control stem cell fate *in vitro* [23,24] and *in vivo* to repair critical-sized bone defects [25]. We have also shown that bBMP-2 presented from a soft film was sufficient to trigger cell spreading and migration [26], overriding the response to film stiffness. The same effect has been shown on rigid surfaces with a low cRGD surface density [27] and on surfaces presenting peptides specific for α5β1 integrins [28]. This process on soft films involved β3 integrins and BMP receptors that worked together to control SMAD signaling and tensional homeostasis[26], thereby coupling cell adhesion and fate commitment. Whether other BMPs are able to induce BMP receptor-integrin crosstalk is poorly known. For instance, BMP-4, which is involved in hematopoiesis, leukemias and cancers [29], is known to induce the expression of α4-integrin [16]. BMP-7 plays a major role in fibrosis, kidney disease and is involved in the adhesion and migration of human monocytic cells [30]. BMP-9 is involved in cardiovascular diseases and anemia [18]. It also increases cell proliferation on bone grafts [31], but its overexpression decreases cell adhesion and migration [32]. However, whether the signaling induced by BMPs is stiffness-dependent, is still elusive.

Recently, we have developed an automated process to deposit the polyelectrolyte films in various multiwell plate formats, especially 96-well microplates [24]. Interestingly, such film-coated microwells enable to study a large number of experimental conditions in parallel.

In addition, multiwell plates are compatible with automated methods to quantify cellular processes using plate readers and automated imaging systems.

In this study, four BMPs including BMP-2, -4, -7 and -9 were selected in view of their physiological importance such as skeletal formation, involvement in cardiovascular diseases, cancers, hematopoiesis and leukemias [2,5,18,29]. All four BMPs have an osteogenic potential *in vitro* [33]. We varied film stiffness to assess the combined effect of bBMP type and substrate mechanics on cell adhesion and differentiation. As BMP-responsive cells, we selected C2C12 skeletal myoblasts [33,34] and human periosteum-derived stem cells (hPDSCs) [35,36] in view of their physiological relevance for bone regeneration and known sensitivity to a large number of BMPs, including these four BMPs [33,37].We directly compared the effect of the four selected BMPs, on stem cell adhesion and early bone differentiation in response to increasing doses of bBMPs presented by the polyelectrolyte film. Cell adhesion, assessed by the number of adherent cells and the cell spreading area, and early bone differentiation, assessed by quantifying SMAD phosphorylation and alkaline phosphatase (ALP) activation, were quantified in an automated manner. Finally, by means of silencing RNA against the type I and II BMP receptors and against three selected β integrins, we identify the roles of each BMP receptor and integrins in cell adhesion, SMAD signaling and ALP expression in BMP ligand- and film stiffness-dependent context.

2 Materials and Methods

2.1 Polyelectrolyte film buildup, crosslinking and BMPs loading

Poly(L-lysine) hydrobromide (PLL) and poly(ethylene imine) (PEI) were purchased at Sigma-Alrich (St Quentin Fallavier, France), and hyaluronic acid (HA) at Lifecore medical (USA). PLL and HA were dissolved in a HEPES-NaCl buffer (20 mM Hepes and 0.15 M NaCl at pH 7.4) at 0.5 mg/mL. PEI was dissolved in a NaCl 0.15 M solution at pH ~6.5, at 4 mg/mL. A first layer of PEI was always deposited. All rinsing steps were performed with 0.15 M NaCl at pH ~6.5. LbL films were directly deposited in 96-well cell culture microplates (Greiner bio-one, Germany) using an automated liquid handling robot (TECAN Freedom EVO® 100, Tecan France, Lyon) and a custom-made macro [24]. The films were then chemically crosslinked using 1-Ethyl-3-(3-Dimethylamino-propyl)Carbodiimide (EDC) at a final concentration of 30 or 70 mg/mL, and N-Hydrosulfosuccinimide sodium salt (Sulfo-NHS) at a concentration of 11 mg/mL as catalyzer, as previously described [38,39]. BMP loading in the films was done following an established protocol [40]. BMP-2 was purchased from Bioventus (France), BMP-4 and -9 from Peprotech (France) and BMP-7 from Olympus Biotech (France).

2.2 Cell culture, and quantification of stem cell adhesion, spreading and differentiation

We used two types of BMP-responsive cells, C2C12 skeletal myoblasts [40] and periosteum-derived stem cells (hPDSCs) [37] to assess the bioactivity of the biomimetic coatings at high content. C2C12 skeletal myoblasts (<15 passages, obtained from the American Type Culture Collection, ATCC) and hPDSC (<12 passages, obtained from F. Luyten) were cultured as previously described [37,40] in tissue culture flasks, in a 1:1 Dulbecco's Modified Eagle Medium (DMEM):Ham's F12 medium (Gibco, Life Technologies, France)

for C2C12 and in high-glucose Dulbecco's modified Eagle's medium (high DMEM) + pyruvate for hPDSC (Gibco, Life Technologies, France), supplemented with 10% fetal bovine serum (FBS, Gibco, Life Technologies, France) and 1% penicillin/streptomycin (Gibco, Life Technologies, France) in a 37 °C, 5% CO_2 incubator. For quantification of cell adhesion and spreading, cells were cultured for 4 or 5 h and then fixed with 4% paraformaldehyde. Nuclei were stained with 4′,6-diamidino-2-phenylindole (DAPI) (Invitrogen, Thermofisher Scientific, France) and the actin cytoskeleton with Alexa Fluor 633-phalloidin (Thermofisher Scientific, France). For analysis of cell adhesion, spreading and pSMAD, 8300 cells/cm^2 of C2C12 and 7000 cells/cm^2 of hPDSCs were seeded in each well.

For quantification of cell differentiation, C2C12 and hPDSCs cells were stained at 4 or 5 h for pSMAD analysis. pSMAD was stained by using a 1:400 dilution of an antibody anti-pSMAD1,5,9 (Cell Signaling, ref: 13820S) or a 1:800 dilution of an antibody anti-pSMAD2 (Cell Signaling, ref: 18338S) both diluted in a solution of bovine serum albumin (BSA, Sigma-Aldrich, Merck, Germany) 3% w/v in PBS. A secondary antibody conjugated to Alexa Fluor 555 (Invitrogen, Thermofisher Scientific, France) diluted at 1:500 in BSA 3% w/v in PBS, was used for both SMAD markers since they were always analyzed in different samples. For the quantification of immunofluorescence stainings, a GE INCA 2500 imaging system (General Electrics Healthcare, France) was used with an inverted 20X objective (Plan Apo N.A.=0.75, Nikon, Japan). 21 images distributed over the well were acquired and, generally, at least 100 cells were analyzed par well and plate. Between 2 and 4 independent experiments (biological replicates) were performed with 2 technical replicates per experiment, making up a total of, generally, at least 400 cells per condition. For comparison of pSMAD1,5,9 and pSMAD2 fluorescent signal, the same exposure time was always used for each marker, which was different between both markers. For image analysis, InCarta software (General Electrics Healthcare, USA) was used to automatically segment nuclei and cells, and to quantify cell number, cell area and pSMAD signal intensity.

For ALP experiments, 15 000 cells/cm^2 were seeded in each wells on rigid films for both cell types, while 33000 cells/cm^2 of C2C12 and 27000 cells/cm^2 of hPDSCs were seeded in each well for soft films. C2C12 cells were stained after three days of culture. hPDSCs were stained after 7 days of culture on soft films and after 14 days on rigid films. The hPDSC cell culture media was carefully changed every three days, and ascorbic acid at 100 μM was added to the hPDSCs culture for cells on soft films. ALP was stained using fast blue RR salt (Sigma-Aldrich, Merck, Germany) in a 0.01 % (w/v) naphtol AS-MX solution (Sigma Aldrich, Merck, Germany), according to the manufacturer's instructions. For C2C12 cells, ALP was imaged using a scanner and quantified using a TECAN Infinite 1000 microplate reader (TECAN France, Lyon) by measuring the absorbance at 570 nm using the multiple-read/well mode [24]. The mean value of 76 measured different positions per microwell was taken. For hPDSCs, ALP was also imaged using a scanner, and the mean grey value for each well of the 8-bit images were calculated with ImageJ.

For quantitative analysis of the BMP dose-response experiments, the data were fitted with an exponential function: $= A_{max} (1- \exp(-[BMP]/Cc))$

Where *Cc* is the characteristic concentration, and A_{max} is the plateau value (in number of cells /mm^2 for the cell number, and in µm^2 for the cell area). In some cases where the curve decayed after reaching a maximum, only the ascending part of the curve was fitted.

In the BMP dose-response experiments, Δ_{max} was calculated by subtracting the maximum value by the value corresponding to the control condition without BMP.

2.3 Expression of BMP and integrin receptors

Expression of BMP type I, type II and integrin receptors was investigated by mRNA transcript analysis. Total RNA from expanded C2C12 and hPDSCs was extracted by lysing cells in lysis buffer supplemented with β-mercaptoethanol. Further RNA extraction was performed using the RNeasy kit (Qiagen) according to the manufacturer's instructions. Complementary DNA (cDNA) was obtained by reverse transcription of total RNA with Oligo (dT)20 as primer (Superscript III; Invitrogen, Thermofisher Scientific, France). Quantitative PCR was performed in duplicates with a thermocycler (MX4800P; Agilent Technologies, France) as previously described [26] using the SYBER green kit. The primer sequences are given in Table SI 2. Primer efficiency was established by a standard curve using sequential dilutions of gene-specific PCR fragments. Data were normalized from the quantitative RT-PCR housekeeping genes EF1, Gusb, and PPIA as an index of cDNA content after reverse transcription.

2.4 Expression of osteogenic, chondrogenic and adipogenic markers

Expression of several markers that are representative of these differentiation pathways were quantified using qPCR. To this end, hPDSCs were cultured in DMEM supplemented with Glutamax, pyruvate, 2% FBS and 1% penicillin/streptomycin for three days. Prior to cell seeding, hPDSCs were first starved for 4h. Cells were then seeded at 45 000 cells/cm^2 on soft and stiff films with bBMPs for three days. RNA was extracted as explained above. The primer sequences are given in Table SI 2.

2.5 SiRNA interference

Cells were transfected with siRNA against β1, β3 or β5 integrins, BMP receptors type I (ALK2, ALK3, ALK5, ALK6), BMP receptors type II (BMPR-II, ACTR-IIA, ACTR-IIB) (ON-TARGET plus SMART pool; respectively, mouse ITGB1, ITGB3, ITGB5, ALK2, ALK3, ALK5, ALK6, BMPR-II, ACTR-IIA, ACTR-IIB) (Dharmacon, France). The gene target siRNA sequences used for transfection are listed in Table SI 3. A scrambled siRNA (Dharmacon, France) was taken as control. Cells were seeded at 5,000 cells/cm^2 in 12-well plates and cultured in 1 ml of GM with 0.5% of antibiotics for 24 h. The transfection mix was prepared as follows: For one well, 2.8 µl of Lipofectamine RNAiMAX Reagent (Invitrogen, Thermofisher Scientific, France) was added to 60 µl of Opti-MEM medium (Gibco, Life Technologies, France) and 1.2 µl of 16.67 µM siRNA, diluted in RNAse free water (5 Prime) was added to another 60 µl Opti-MEM medium. Lipofectamine-containing mix was added to siRNA-containing mix and incubated for 20 min at RT. Then, 120 µl of the final mix was added to each well. After 24 h of incubation at 37°C, the cells were transfected for the second time and incubated for another 24 h. The cells were then detached

with 0.25% trypsin-EDTA (Gibco, Life Technologies, France), seeded in GM on the films, and allowed to adhere.

2.6 Data representation and statistical analysis

For box plots, the box shows 25, 50 and 75% percentiles, the square shows the mean value and the error bars correspond to the standard deviation. For scatter plots and bar plots, the mean values and the standard error of the mean (SEM) are represented. Experiments were performed in duplicate, triplicate, or quadruplicate (biological replicates) with 2 wells per condition (technical replicate) in each experiment. Statistical analysis was performed using the non-parametric analysis Kruskal-Wallis analysis of variance (K-W ANOVA) to obtain p values ($p < 0.05$ was considered significant).

In the adhesion and spreading experiments, the mean values of cell number and cell area were obtained by averaging all the values for all the wells (technical and biological replicates). To calculate the mean value of pSMAD signal, first the average of all values per well was calculated, then the average of all wells from all the experiments was calculated. In the ALP experiments for C2C12 cells, the mean value was obtained by averaging the mean absorbance values of each well from all the experiments. In the same experiments for hPDSCs, the mean value was obtained by averaging the mean grey values of each well from all the experiments. To obtain normalized gene expression fold increase of the hPDSCs markers, firstly the mean gene expression values, previously normalized by the reference genes, of each experiment (generally 3 technical replicates) was calculated. Then, for each experiment, values were normalized by the value of the condition “soft film with no BMP”. Finally, the mean value and the SEM were calculated from 2 to 3 experiments. In the knockdown experiments, the relative values were calculated by first averaging all the mean values per well from all the experiments, then normalizing the values by the scrambled condition.

3 Results

3.1 Cell adhesion and spreading of C2C12 and hPDSCs are induced in a BMP-specific and stiffnessdependent manner

To investigate whether the film stiffness may affect the effect induced by the four BMPs, namely BMP-2, -4, -7 and -9, in early cell adhesion and spreading we bound them non-covalently to a polyelectrolyte film of controlled stiffness made of poly(L-lysine) (PLL) and hyaluronic acid (HA) [14],[26],[38]. The polyelectrolyte films were crosslinked to different levels using a crosslinker EDC, as previously described [38], which leads to low and high crosslinked films (EDC30 and EDC70, respectively), named hereafter for simplicity soft (S) and rigid (R) films. Their stiffness corresponds to ~200 kPa (soft) and ~400 kPa (rigid) [38]. The amounts of the four BMPs loaded in the films were quantified (Table SI 1). BMP-2, -4, -7, and -9 could all be loaded in the films at 65 to 95% of the loading concentration depending on the BMP type, with only slight stiffness-differences. Surprisingly, BMP-9, which is known to be found circulating in plasma in soluble form [41], was well bound to the matrix, with incorporation percentages of 92 and 88% on soft and rigid films,

respectively. Thus, the four BMPs could be presented to cells in a matrix-bound manner (bBMPs).

Cells were fixed and analyzed 4-5 h after cell seeding to enable cell adhesion and spreading on the soft and stiff films. Both cell processes are usually slower on the films than on tissue culture polystyrene or glass, both of which are orders of magnitude stiffer than the films [23]. Soluble BMPs (sBMPs) in the cell culture medium were used as control, at a constant concentration of 200 ng/ml, which is considered as a high concentration [23].

Cells were cultured on soft and rigid films with increasing concentrations of bBMPs, obtained by loading the films with BMP solutions from 0 to 20 μg/mL. Representative images of cell adhesion are given in Fig. 1A and Fig. SI 1, together with the quantification of the number of adherent cells (Fig. 1B) and cell spreading areas (Fig. 1C). At first sight, it appears that the cells adhere and spread on all bBMPs in a concentration-dependent and stiffness-dependent manner, whatever the bBMPs, except on soft films with bBMP-9. After quantitative analysis, we observe that cell number and cell area values are generally higher on rigid films than on soft ones (Fig. 1B and C). However, on the non-BMP condition, this increase is only observed for cell number but not for cell spreading.

The quantified data were fitted with an exponential function toward a plateau value (see Methods) and two quantitative parameters were extracted: Δ_{max} (difference between the highest value and value for the no BMP condition) and 1/Cc (Fig. 1D-G). Cc (in μg/mL) corresponds to the characteristic concentration extracted from the exponential fit of the data. It corresponds approximately to the BMP concentration when half of the plateau value is reached. 1/Cc provides a direct quantification of the cell sensitivity to bBMPs: the higher it is, the higher is the sensitivity to a given bBMP. Regarding Δ_{max}, the higher it is, the stronger is the effect for a given BMP.

The increase in cell number (Δ_{max}) was stiffness-dependent for bBMP-4 and -7, being higher on soft than on rigid films (Fig. 1D). In cell area, this same parameter was found to be stiffness-dependent for all the bBMPs. However, the increase in cell area was always higher on rigid films than on soft ones (Fig. 1F). Regarding the sensitivity parameter (1/Cc), it was stiffness-sensitive for bBMP-2 and -4 in cell number (Fig. 1E), and for bBMP-2, -4 and -7 in cell area (Fig. 1G), being in all cases higher on rigid films than on soft ones. However, a rather large standard deviation was found for bBMP-7 sensitivity parameter on cell area. bBMP-9, in particular, only helped increasing adhesion and spreading on rigid films and no response was observed on soft ones at this time scale (Fig. 1B and D), indicating a smaller role on adhesion and spreading of this bBMP in comparison to the others.

Interestingly, plotting the data in relative percentage compared to the no BMP condition, further highlighted the fact that soft films with bBMPs had a stronger role on cell adhesion than rigid films, while rigid films with bBMPs had a stronger role on cell spreading (Fig. SI 2). Soluble BMPs (sBMPs) added on cells cultured in the same experimental conditions than with bBMPs, only had an effect increasing cell area on rigid films with sBMP-2 (Fig. SI 3), confirming that bBMPs amplify cell adhesive response.

The adhesive response of hPDSCs (Fig. SI 4 and SI 5) was qualitatively and quantitatively similar to that of C2C12 myoblasts. However, we noted some differences: regarding the Δ_{max} value, cell adhesion was stiffnessdependent for all four BMPs (Fig. SI 3) while the cell area was only stiffness-dependent for bBMP-4 and higher on soft than on rigid films (Fig. SI 3G). Regarding the kinetics, faster adhesion kinetics were observed on rigid films with bBMP-7 in comparison to soft ones (Fig. SI 3F and H), while no stiffness-dependent differences were observed on C2C12 cells. We also noted that, on rigid films with bBMP-2, bBMP-7, and to a lesser extent with bBMP-4, the cell number and cell area values, decreased after reaching the maximum value, showing a dual response of hPDSCs to high bBMP concentrations. Finally, on bBMP-9, contrary to C2C12 cells, very small adhesion could be measured on soft films (Fig. SI 3B). As with C2C12, data in relative percentage further highlighted the fact that soft films with bBMPs had a strong role of both cell adhesion and spreading of hPDSCs (Fig. SI 5). Here again, this effect was specific to bBMPs since sBMPs only had an influence increasing cell area on rigid films with sBMP-2 (Fig. SI 6).

Altogether, our data showed that the four studied bBMPs positively act either on the cell number, on the spreading area or both. There is BMP-specific response to film stiffness. The increase in cell number thanks to bBMPs was stronger on soft films than on rigid ones, notably for BMP-4 and -7, while cell area was more strongly enhanced by bBMPs on rigid than soft films. In general, cells respond faster, in terms of adhesion and spreading, on rigid films than soft ones. Similar behaviors were observed between C2C12 cells and hPDSCs.

3.2 Early stem cell differentiation in bone is BMP-specific and stiffness-dependent

SMAD1,5,9 is a transcription factor known to play a key role in the transduction pathway from BMP receptors to the nucleus [42] and its phosphorylation is often taken as readout of early cell differentiation [42]. While SMAD2,3 is described as being triggered mainly by TGF-βs and activins [43], it was also shown to be triggered by sBMPs [44]. We decided to include it in our study and quantify the phosphorylation of the nuclear translocated SMAD2. One of the markers for the so-called non-canonical pathway is the induction of alkaline phosphatase (ALP) [42], which is often taken as later osteogenic readout [33].

We then studied the phosphorylation and nuclear translocation of SMAD1,5,9 and SMAD2 after 4-5 h of culture on the films with increasing BMP concentrations (Fig. 2, Fig. SI 8). In order to avoid differences in fluorescent signal intensity between experiments, we normalized the fluorescent signals of pSMAD1,5,9 and pSMAD2 of each experiment by the non-BMP condition (Fig. 2A and D). Not-normalized data is shown in Fig. SI 8. Representative examples of pSMAD fluorescent signal values distribution, together with representative pictures of C2C12 cells presenting low and high pSMAD signals, are shown in Fig. SI 7.

After fitting the curves, as we did with cell adhesion and spreading, and extracting the parameters Δ_{max} and 1/Cc, we observed that, for pSMAD1,5,9 Δ_{max} value was higher on soft than on rigid films with bBMP-2, -4 and -7 (Fig. 2B). The sensitivity value (1/Cc) instead, was higher on soft than on rigid films with bBMP-2 and -4, but it was stiffness-independent for bBMP-7, which gave the lowest sensitivity. Nevertheless, attention should

be paid due to big error bars (Fig. 2C). Curiously, at lower bBMP-7 concentrations on rigid films, the pSMAD1,5,9 values were below that of the non-BMP condition (Fig. 2A and SI 8A). Regarding bBMP-9, the cell response could solely be measured for cells cultured on stiff films, since C2C12 cells were barely adhering after 5 h on the soft films. bBMP-9 induced a high pSMAD1,5,9 response (Fig. 2A and SI 8A), with a high sensitivity (Fig. 2C). To note, pSMAD1,5,9 response to sBMPs was solely increased for cells on stiff films with sBMP-2 and 9 (Fig. SI 9).

pSMAD2 signal was stiffness-independent in all conditions except for cell sensitivity parameter (1/Cc) with bBMP-4, where soft films induced a higher sensitivity than rigid ones. However, the error bar in this condition was big (Fig. 2F). bBMP-9 triggered the strongest pSMAD2 signal, followed by bBMP-2 (Fig. 2D-F and Fig. SI 8B). bBMP-4 induced a higher pSMAD2 than pSMAD1,5,9 signal in terms of Δ_{max} on both film rigidities (Fig. 2E), and sensitivity only on rigid films (Fig. 2F). Similarly, to pSMAD1,5,9, at low concentrations bBMP-7 induced slightly smaller pSMAD2 signal values than the control, but on soft films instead (Fig. 2D and Fig. SI 8B).

The ALP response of C2C12 cells was quantified after 3 days of culture [24]. The results corresponding to rigid films were extracted and adapted from P. Machillot *et al.* [24]. Here, cells on soft films with bBMP-9 could be analyzed, since they could better adhere after 3 days of culture. bBMP-2 and bBMP-9 exhibited a strong stiffness-dependent response, with a significantly higher ALP activation on rigid films than on soft ones (Fig. 2G-I and Fig. SI 10). Conversely, the ALP response to bBMP-4 and -7 was very high for both soft and stiff films with only little stiffness-dependence (Fig. 2G-I). The ALP response to bBMP-4 and -7 on soft films was also higher than that to bBMP-2 and -9. Generally, for the ALP response, the sensitivity of cells to bBMPs was higher on rigid films (Fig. 2I).

Regarding the osteogenic differentiation of hPDSCs, we studied pSMAD1,5,9 and ALP response to the four bBMPs (Fig. SI 11). pSMAD1,5,9 was found to be stiffness-dependent for bBMP-2, 4 and 7 with a higher signal for cells on soft films with bBMPs. Regarding the ALP response, it was also stiffness-dependent notably for bBMP-2 and 4. The ALP response to bBMP-7 and bBMP-9 was low, with, here again, a slightly higher response for cells on soft films with bBMPs. The results corresponding to rigid films were extracted and adapted from P. Machillot *et al.* [24].Altogether, our data for C2C12 and hPDSCs cells showed BMP-specific and stiffness-dependent responses. For bBMP-2, ALP response was stiffness-dependent and pSMAD1,5,9 signal was also stiffness-dependent, but to a lower extent. bBMP-4 induced a strong ALP response whatever the film stiffness and also induced to a lower extent pSMAD1,5,9 and pSMAD2 signals. bBMP-7 also strongly activated ALP, to a lower extent pSMAD1,5,9 and even less pSMAD2. Lastly, from all the four BMPs, bBMP-9 induced the highest SMAD response and a very high ALP response. In striking contrast, bBMP-9 did not induce ALP expression in hPDSCs.

3.3 bBMPs can also induce other non-osteogenic differentiation pathways in hPDSCs

In order to investigate whether hPDSCs may undergo other differentiation pathways, we studied the expression of several genes that are representative of the osteogenic, chondrogenic and adipogenic differentiation. To this end, we selected as osteogenic markers

osterix, DLX5, osteopontin, as chondrogenic markers sox9, Aggregan, Col2A1, and as adipogenic markers PPARγ, C/Ebp a, adiponectin [45]. Gene expression was assessed for hPDSCs after three days of culture (Fig. 3). Regarding the osteogenic markers, bBMP-2 and 9 induced osterix, DLX5 and osteopontin expression, but the effect was stronger for bBMP-9. This osteogenic induction was stiffness-dependent, with higher gene expression on soft films with bBMP-2 and 9 in comparison to rigid ones (Fig. 3A-C).

Regarding the chondrogenic markers, aggrecan was strongly expressed in cells grown on rigid films with bBMP-2. Conversely, aggrecan was slightly higher for cells on rigid films with bBMP-7 than for those on soft ones. In contrast to the other bBMPs, bBMP-9 induced a strong inhibition of aggrecan expression. Interestingly, this same BMP, induced an antagonistic stiffness-dependent expression of col2A1: on soft films it is an inhibitor and on rigid films an activator (Fig. 3D-F).

Regarding the adipogenic markers, PPARγ was increased on rigid films without BMPs and was strongly decreased on bBMP-9 irrespective of the film stiffness. C/Ebp was strongly increased solely on soft films with bBMP-2. Adiponectin was also expressed in a stiffness-dependent manner in response to bBMP-2: it increased on soft films with and, conversely, decreased on rigid films. Regarding bBMP-9, rigid films induced a decrease in the expression of adiponectin (Fig. 3G-I).

Thus, bBMP-2 and bBMP-9 appear to be not only the best activators of the osteogenic pathways, but also to play a role in the chondrogenic and adipogenic pathways. This stiffness-dependent role was bBMP- and marker-specific.

3.4 Involvement of BMP receptors and integrins in the cell adhesive response

Having evidenced that bBMPs can act as adhesive molecules to trigger myoblast and periosteum stem cell adhesion and spreading, we aimed to unravel the specific role of the BMP receptors and of integrins in the cell adhesive response. Firstly, an *in silico* screening was performed using RNA sequencing data from UCSC genome browser (Encode database). Thus, we identified the adhesion receptors expressed in C2C12 cells and expressed their relative abundance by quantifying the percentage (Fig. SI 12). We then verified the expression level of the BMP receptors (BMPR) and integrins of C2C12 myoblasts and hPDSCs using quantitative PCR (Fig. 4A and B). For C2C12 myoblasts, mRNA transcripts for the type I BMPR, ALK2, ALK3 and ALK5 were detected. ALK1, ALK4 and ALK6 were expressed at a much lower level. For the type II BMP receptors, BMPR-II, ACTR-IIA and to a much lower extent ACTR-IIB were detected. Regarding integrins, in both cell types β1 was the most highly expressed followed by β5 and β3. For hPDSCs, the similar BMP type I, II and integrins were detected, although their expression was quantitatively lower.

Next, we quantified the molecular interactions between the four BMPs and the BMP receptors type I and II using reflectometric interference spectroscopy with the commercially-available biolayer interferometry setup. We obtained the affinity constants (Kd) values for each BMP-BMP receptor couple (Fig. 4C), as recently shown in Khodr *et al.* [46]. Confirming the literature data [4], BMP-2 and BMP-4 exhibited high affinity for ALK3 and ALK6. BMP-7 exhibited a different behavior since it has the highest affinity for ACTR-IIA

and has a moderate, non-specific affinity for all ALK receptors. BMP-9 had the strongest affinity for ALK1 and a similar affinity for the three type II receptors. We did not consider ALK4 for this study since it is an activin receptor and no evidence was found in the literature regarding a possible interaction with BMPs.

In order to assess the specific role of each receptor, type I (ALK2, 3, 5 and 6) and type II BMP receptors (BMPR-II, ACTR-IIA, ACTR-IIB), as well as β integrins (1, 3 and 5) were silenced using siRNA. The efficacy of the silencing was first verified (Fig. SI 13). The cell number and cell spreading area were analyzed on one particular BMP concentration (20 μg/ml), normalized by the scrambled control condition and averaged, to reveal the contribution of each receptor (Fig. 5 and Fig. SI 14). Non-normalized raw data are plotted in Fig. SI 15.

Among the ALK receptors, on the no BMP condition, ALK3 had the greatest impact, influencing cell adhesion and spreading area, while ALK5 had an effect on cell spreading. ALK6 had two opposites effect, being an activator of cell adhesion and an inhibitor of cell spreading (Fig. SI 14).

In the cell response to bBMPs (Fig. 5), ALK3 had a stiffness-dependent role on bBMP-2 and 4, which was also “readout-dependent”. Thus, ALK3 enhanced cell spreading for bBMP-2 in a stiffness-dependent manner, but there was no stiffness-dependence on cell number. Conversely, ALK3 played a stiffness-dependent role for cell adhesion on bBMP-4 but it induced cell spreading independently of film stiffness with this same BMP. ALK2 had a minor role on cell number but a significant stiffness-dependent role on cell area, notably for bBMP-2: it activated cell spreading on soft films and inhibited cell spreading on stiff films. ALK5 was involved in a mechano-sensitive cell adhesion on bBMP-4 and -7, being an inhibitor on soft films and an activator on rigid ones (Fig. 5A and Fig. SI 15A). ALK5 also had a stiffness-dependent role in cell spreading, in response to bBMP-2, with a stronger activation role on soft films than on rigid ones. ALK6 promoted adhesion but inhibited cell spreading even in the absence of BMP (Fig. SI 14). When bBMPs were present, ALK6 induced adhesion only on rigid films but not on soft ones (Fig. 5), while it was an inhibitor of cell area on bBMP-2, 7 and 9.

Regarding type II BMP receptors, mainly BMPR-II and ACTR-IIA played a certain role in adhesion and spreading. On the non-BMP condition, both receptors induced adhesion, while BMPR-II inhibited spreading and ACTR-IIA activated it (Fig. SI 14). On films with bBMPs, BMPR-II was a slight inhibitor of cell spreading, but a strong activator of cell adhesion on soft films with bBMP-2. ACTR-IIA was mechanosensitive, being an inhibitor of cell adhesion on soft films with bBMP-4 and -7, and activator on rigid films in response to all BMPs. It had a minor role on cell spreading, except for rigid films with bBMP-9 where it induced cell spreading (Fig. 5).

With respect to integrins, β3 integrin had an important and consistent role in activating both cell adhesion and spreading, independently of film stiffness and of the presence of BMPs. The role of βl integrin was generally comparable to that of β3. β1 integrin was also involved in a mechano-sensitive response to bBMP-7, acting as an inhibitor of cell adhesion on soft films, and an activator on rigid ones. Lastly, β5 integrin was involved in a mechano-sensitive

Europe PMC Funders Author Manuscripts

cell response to bBMP-2: it was an inhibitor of cell adhesion on soft films and no role on rigid ones. β5 integrin was an inhibitor of cell spreading on bBMP-2 and -4, on both film stiffness, and on soft films with bBMP-7 (Fig. 5 and Fig. SI 14).

3.5 Involvement of BMP receptors and integrins in early cell differentiation to bone

The effect of receptor silencing on early osteogenic differentiation was also investigated for pSMADs and ALP activity (Fig. 6 and Fig. SI 16). Non-normalized raw data are plotted in Fig. SI 17.

Regarding pSMAD1,5,9, ALK2 exhibited an important role for all BMPs in a non-specific manner. ALK3 revealed to have a BMP-specific role: it is an activator for bBMP-4 and an inhibitor for bBMP-7 and -9. ALK6 was an activator of pSMAD1,5,9 on all bBMPs. ALK5 had only a minor inhibiting role for bBMP-2, -4 and - 7, which was more visible on soft films than rigid ones (Fig. 6A).

With respect to the BMPR type II receptors, BMPR-II was an important and a non-specific activator for all BMPs on both film stiffness, as well as for the no BMP condition (Fig. 6A and Fig. SI 16A), while ACTR-IIA was an activator of the pSMAD1,5,9 response to bBMP-7, independently of film stiffness.

Lastly, β integrins were found to have a minor role on SMAD1,5,9 activation in comparison to ALKs and BMP-type II receptors. β3 integrin was the most important activator, notably for bBMP-2 and -4, on both film stiffness, and solely on soft films for bBMP-7. β5 integrin had a minor inhibiting role on soft films with bBMP-4 and -7, and on rigid films with bBMP-9 (Fig. 6A).

For pSMAD2 (Fig. 6B), BMPR-II was again an important and non-specific activator for all bBMPs, and the no BMP condition (Fig. SI 16), especially on rigid films. Interestingly, here again, ALK3 had a notable role: being a stiffness-dependent activator for the pSMAD2 response to bBMP-4, a stiffness-dependent inhibitor for the response to bBMP-7, and an inhibitor for bBMP-9, its role being prominent on rigid films in comparison to soft ones.

Regarding the ALP activity (Fig. 6C and Fig. SI 17, 18), generally, ALK2, ALK3 and ALK6 were activators, whereas ALK5 had only an inhibitor role for bBMP-2 (Fig. 6C). BMPR-II and ALK6 played the most important role in activating ALP. However, ALK6 was a stronger ALP activator than BMPR-II on bBMP-2, -4 and -7 for soft films, and on bBMP-9 for rigid ones. ACTR-IIA played a role in ALP activation on bBMP-4 and -7, independently of film stiffness. ACTR-IIB only played a minor role inhibiting ALP on bBMP-2 (Fig. 6C). Regarding integrins, β3 and β5 integrins were generally activators of ALP for bBMP-2, -4 and -7. β1 integrin was rather inhibiting ALP notably on soft films and had almost no effect on stiff films, except for BMP-2 (Fig. 6C).

Globally, the role of the receptors was related to each readout of the osteogenic differentiation (pSMAD1,5,9; pSMAD2 or ALP) with only little differences depending on the film stiffness, and little differences between the bBMPs except for the ALK3 and ACTR-IIA receptors.

Table 1 summarizes the role of each BMP receptor and integrin receptor for all the readouts studied in cell adhesion and cell differentiation. In this table, we distinguished whether the role of the receptor was stiffnessdependent or stiffness-independent.

4 Discussion

4.1 Stiffness dependence of BMPs and BMP receptors in cell adhesion, spreading and cell fate commitment

For the first time, the effect of 4 different BMPs, presented in a matrix-bound manner, has been compared on cell adhesion, spreading, SMAD signaling, ALP activity and capacity to induce other differentiation pathways (i.e. chondrogenesis and adipogenesis). We show that, generally, film stiffness plays a relevant role on the BMP-induced cell responses. Regarding osteogenic differentiation, when looking further at osteogenic markers, we found that bBMP-2 and 9 are the most potent inductors, and that soft films with bBMPs are the most favorable surfaces to trigger the expression of the bone markers, in comparison to stiff ones. bBMP-2 had a notable effect on aggrecan expression while bBMP-9 induced a strong increase in Col2A1, these phenomena being again favored by film softness. To note, adipogenic markers where also increased on soft films with bBMP-2, while they were downregulated on stiff films with bBMP-2, highlighting the stiffness-dependent response to bBMP-2 in adipogenesis. Globally, stiff films with bBMP-9 were the most potent inhibitors of adipogenesis. In fact, the capacity of hPDSCs to engage cell fate towards chondrogenesis and adipogenesis has already been shown, by tuning cell adhesion strength, cell contractility, and mechanical cues, but without using BMPs [45]. In this study, they also used differentiation media specific for each lineage, and they observed cell differentiation after 1-2 weeks. The fact that we present BMPs in a matrix-bound form, may accelerate the time to induce lineage-specific markers expression down to 3 days. In a different study, adipogenic differentiation with human Bone Marrow Stem Cells was observed using human recombinant BMP-2 in soluble form [47]. Yet in another study, where BMP-4 and 9 were administrated via calcium phosphate scaffolds, no induction of osteogenic nor chondrogenic markers was observed, probably due to an inappropriate calcium stimulation leading to inhibition [37].

Our high-content study could be done thanks to a recently-developed automated procedure to deposit the biomimetic films directly in 96-well cell culture microplates [24]. Automation increases the reproducibility of film deposit and the film-coated plates can be used to parallelize the experiments and study several experimental conditions simultaneously. In addition, optimizing image acquisition and subsequent quantitative analysis enabled to characterize early cell adhesion and differentiation with different readouts.

We revealed that all four studied bBMPs are able to induce both cell adhesion and spreading (Fig. 1, Fig. 6 and Fig. SI 2, 4 and 5). This finding greatly extends our initial findings regarding the role of bBMP-2 on cell adhesion and migration [23]. The unique effect of BMPs on cell adhesion and spreading could be revealed thanks to the matrix-bound presentation of the BMPs together with the modulation of film stiffness, soft films revealing the most striking BMP-specific differences. Among the four studied BMPs, bBMP-4 and bBMP-7 induced the most potent cell adhesion and spreading for both C2C12 myoblasts and

hPDSCs (Fig. 1D-G and Fig. SI 4D-G). With C2C12 cells, all four bBMPs had a stronger role inducing cell spreading on rigid films than on soft ones (Fig. 1F and G). However, in the absence of BMP (no BMP condition), only the cell number increased on rigid films with respect to soft ones, but not cell spreading, in contrast to what has been found in previous works [23,26]. bBMP-9 on soft films was not sufficient to induce a strong cell adhesion nor cell spreading with C2C12 myoblasts (Fig. 1B and C), while it induced a small increase with hPDSCs (Fig. SI 4B-D and F). The fact that BMP-9 does not bind to ALK3 and ALK6 may explain this result, since these two receptors were found to be important for cell adhesion (Fig. 5A). In addition, ALK3 was also found to be important in cell spreading (Fig. 5B). Our data are consistent with other studies showing a positive effect of BMP-2, -4 and -7 on cell adhesion and migration with other cell types [26,30,48].

Furthermore, we revealed the specific roles of BMPR type I, type II, and three β-chain integrins, on the aforementioned cell responses, which are context-specific and BMP-dependent.

ALK2 appears to be mechano-sensitive in response to bBMP-2 only (Fig. 5), by inducing cell spreading on soft films. Our data are consistent with the recently reported mechanosensitivity of ALK2 [49]. Interestingly, this mechanosensing appears to be altered during heterotypic ossification associated to fibrodysplasia ossificans progressiva (FOP).

ALK3 appears to be a central receptor in cell adhesion and spreading for all BMPs (Fig. 5 and Fig. 7C). ALK3 has a major role in several cancers [5] and plays a role in the adhesion of human epithelial ovarian cancer spheroids to the substratum [50].

We found that ALK5 tends to be mechano-sensitive for cell spreading on bBMP-2, and for cell adhesion on bBMP-4 and 7 (Fig. 5 and Fig. 7C). Our data are consistent with the role of ALK5 described in other contexts showing a mechanosensing role of this receptor. In fact, ALK5 is historically known as a TGF-β receptor [51] and for its involvement in EMT in breast epithelial [52] and endothelial cells [53]. It was already shown to be involved in the response to shear stress in the endothelium [54], in chondrocyte mechanosensing [55] and in the activation of focal adhesion kinase (FAK) in lung epithelial cells [56].

Our data revealed an important mechano-sensitive role of ACTR-IIA in cell adhesion, notably in response to both bBMP-4 and bBMP-7 (Fig. 5A and Fig. 7D). This finding is in line with a work showing a mechano-sensitive role of ACTR-IIA in tenogenic commitment of adipose stem cells under magnetic stimulation [57].

4.2 Identification of integrins in BMP-induced cell adhesion, spreading and BMP signaling

Regarding the role of integrins, β3 integrin appears to have a major role in cell adhesion and spreading on all bBMPs. The role of β3 integrins is crucial for cell adhesion in soft environment, which corresponds to our finding, whereas both β1 and β3 integrins cooperate in a stiff environment as already described [58]. β1 integrin was also important for cell adhesion and spreading on all bBMPs, with a peculiar stiffness-dependent response for cell

adhesion to bBMP-7. β5 integrin also exhibited a stiffness-dependent response to bBMP-2 and to a lower extent to bBMP-4 (Fig. 5 and Fig. 7E).

Apart from their role in adhesion and spreading, integrins are also important for bone differentiation [59]. In our experimental conditions, we found that βl integrin is a slight inhibitor of BMP-2-mediated C2C12 ALP activity for soft and stiff films, while it was stiffness-dependent on bBMP-7 (Fig. 6C and Fig. 7E). The role of β1 integrin in osteoblastic differentiation is already recognized, but appears to be cell-type and context-specific. A previous study in our team by Sefkow-Werner *et al.* [27], using C2C12 myoblasts, revealed an activator role of β1 integrin with sBMP-2 and BMP-2 bound to heparan sulfate. Many data have shown that β1 integrin plays an important role in osteoblast differentiation and function [60–62]. Mice expressing a dominant-negative β1 integrin in mature osteoblasts show reduced bone mass and defective bone formation [60]. β5 integrin has been shown to be involved in bone differentiation in a non-SMAD-dependent manner [63].

4.3 Stiffness dependence of BMP and BMP receptors in SMAD and ALP signaling

BMPs are traditionally referred to activate the pSMAD1,5,9 pathway [43] whereas TGF-β activates SMAD2,3 signaling [51]. To our knowledge, to date, there was no systematic comparison of the role of BMPs on SMAD and ALP signaling available in the literature. Here, we showed that all four bBMPs are able to activate both pSMAD1,5,9, pSMAD2 and ALP pathways in a BMP-specific and, in certain conditions, in a stiffness-dependent manner (Fig. 7A and B, and Table 1). As far as film stiffness is concerned, pSMAD1,5,9 and pSMAD2 Δ_{max} values were always higher on soft films (Fig. 2A, B, D, and E). Notably, bBMP-4 induced a negligible pSMAD1,5,9 response on stiff films while bBMP-9 induced the highest one.

Indeed, BMP-2 was recently shown to promote both canonical SMAD1,5,8 and non-canonical SMAD2,3 pathways in trophoblast cells [64]. Soluble BMP-4 also activates SMAD3 [65]. Our data is also consistent with SMAD and non-SMAD signaling reported for BMP-7 induced BMP signaling in tenocyte-like cells [66].

Regarding pSMAD1,5,9 signaling, ALK2 and ALK6 were found to have a central role independently of the BMP type, while the effect of ALK3 was bBMP-specific: it is a strong activator on bBMP-4 and inhibitor on bBMP-7 and -9 (Fig. 6A and Fig. 7C).

BMPR-II had a major activator role for all bBMPs while ACTR-IIA was specifically associated to the response to bBMP-7 (Fig. 6A and Fig. 7D). Our data are consistent with the role of ACTR-IIA for BMP7-mediated chemotaxis of monocytes and pSMAD activation [67].

The important role of bBMP-9 activating SMAD1,5,9 and SMAD2, may be related to the strong binding to BMPR-II (Fig. 4), which plays a key role in SMAD activation (Fig. 6A and D), and to ALK1 (Fig. 4) which is also important for SMAD2,3 and SMAD1,5 activation [68]. The fact that BMP-9 is not sensitive to the BMP inhibitor Noggin may also contribute to the strong SMAD activation [69].

ALP is a common marker to assess BMP-induced osteoblastic differentiation [33]. We showed that ALP is highly activated in C2C12 cells in response to bBMPs (Fig. 2G and Fig. SI 10). Our data are in agreement with the previously demonstrated ALP activities evidenced for soluble BMP-2, -4, -7, and -9 [33]. We showed here for the first time a BMP-specific stiffness-dependent ALP response of cells cultured on bBMPs. Indeed, ALP was stiffness-dependent in response to bBMP-2 and -9 and stiffness-independent for bBMP-4 and -7 (Fig. 2G-I). The relevant roles of ALK2 and ALK3 in ALP activation that we observed, are consistent with role of ALK2 in ALP activity [70] as well as the role of ALK3 [71], found in the literature. Interestingly, ALK6 was a strong ALP activator despite its low level of expression on C2C12 cells (Fig. 6C and Fig. 7C). As with SMAD proteins, BMPR-II played a crucial role activating ALP. Our data also showed that ACTR-IIA is an activator of BMP-4 and 7-mediated ALP activity, while ACTR-IIB was an inhibitor solely for the ALP response to bBMP-2 (Fig. 6C). They are consistent with the role of ACTR-IIA and B receptors in the regulation of bone mass [72].

5 Conclusions

In this work, we carried out for the first time an extensive study on the effects of matrix-bound BMPs on cell adhesion and differentiation. We revealed the effect of four matrix-bound BMPs combined with two film rigidities (soft and rigid), on early steps of cell mechanotransduction and differentiation for two cells types, C2C12 skeletal myoblasts and human periosteum derived stem cells. In addition, using siRNA, we revealed the unique roles of type I and type II BMP receptors, as well as of three beta chain integrins, on cell adhesion (cell number and spreading) and bone differentiation. We found that several receptors act in a stiffness-dependent manner, which is also BMP type-dependent and readout-dependent. This high-content study paves the way for future signaling studies, in particular cellular and tissue contexts, to elucidate the specific roles of BMPs and TGF-β growth factors, matrix stiffness, BMP receptors and cell adhesion receptors. In view of the important roles of BMPs in physiological and pathological processes, such studies will enable to better understand the underlying signaling mechanisms and, ultimately, to propose new treatments of BMP- and TGF-β-related diseases.

Supplementary Material

Refer to Web version on PubMed Central for supplementary material.

Acknowledgements

C. Picart is a senior member of the Institut Universitaire de France, whose financial support is acknowledged. The study was supported by Agence Nationale de la Recherche (ANR CODECIDE, ANR-17-CE13-022 to C.A.R. and C.P, ANR GlyCON, ANR-19-CE13-0031-01 E.M.), by the Fondation Recherche Medicale (FRM) (grant DEQ20170336746 to C.P. DEQ20170336702 to C.A.R), by the European Research Council (ERC Biomim, GA 259370, POC BioactiveCoatings, GA692924). We are part of the GDR2088 “BIOMIM” and the GDR “Réparer l’humain” research networks. V.K. was supported by a PhD fellowship from Grenoble Institute of Technology. A. Guevara-Garcia was supported by a CONACYT fellowship from the mexican government (CVU: 532484). We thank Prof. Franck Luyten for providing the hPDSCs cells and for fruitful discussions. We are grateful to David Pointu for his technical advices.

Data availability statement

The raw and processed data required to reproduce these findings are available upon request to Catherine Picart and/or Adrià Sales.

References

[1]. Massagué J. How cells read TGF-β signals. Nat Rev Mol Cell Biol. 2000; 1: 169–178. DOI: 10.1038/35043051 [PubMed: 11252892]

[2]. Wagner DO, Sieber C, Bhushan R, Börgermann JH, Graf D, Knaus P. BMPs: From bone to body morphogenetic proteins. Sci Signal. 2010; 3: 1–7. DOI: 10.1126/scisignal.3107mr1

[3]. Salazar VS, Gamer LW, Rosen V. BMP signalling in skeletal development, disease and repair. Nat Rev Endocrinol. 2016; 12: 203–221. DOI: 10.1038/nrendo.2016.12 [PubMed: 26893264]

[4]. Ehata S, Yokoyama Y, Takahashi K, Miyazono K. Bi-directional roles of bone morphogenetic proteins in cancer : Another molecular Jekyll and Hyde ? Pathol Int. 2013; 63: 287–296. DOI: 10.1111/pin.12067 [PubMed: 23782330]

[5]. Jiramongkolchai P, Owens P, Hong CC. Emerging roles of the bone morphogenetic protein pathway in cancer: Potential therapeutic target for kinase inhibition. Biochem Soc Trans. 2016; 44: 1117–1134. DOI: 10.1042/BST20160069 [PubMed: 27528760]

[6]. da Silva Madaleno C, Jatzlau J, Knaus P. BMP signalling in a mechanical context - Implications for bone biology. Bone. 2020; 137 115416 doi: 10.1016/j.bone.2020.115416 [PubMed: 32422297]

[7]. Antebi YE, Linton JM, Klumpe H, Bintu B, Gong M, Su C, McCardell R, Elowitz MB. Combinatorial Signal Perception in the BMP Pathway. Cell. 2017; 170: 1184–1196. e24 doi: 10.1016/j.cell.2017.08.015 [PubMed: 28886385]

[8]. Morikawa M, Derynck R, Miyazono K. TGF-β and the TGF-β family: Context-dependent roles in cell and tissue physiology. Cold Spring Harb Perspect Biol. 2016; 8 doi: 10.1101/cshperspect.a021873

[9]. Sedlmeier G, Sleeman JP. Extracellular regulation of BMP signaling: welcome to the matrix. Biochem Soc Trans. 2017; 45: 173–181. DOI: 10.1042/BST20160263 [PubMed: 28202671]

[10]. Ramel MC, Hill CS. The ventral to dorsal BMP activity gradient in the early zebrafish embryo is determined by graded expression of BMP ligands. Dev Biol. 2013; 378: 170–182. DOI: 10.1016/j.ydbio.2013.03.003 [PubMed: 23499658]

[11]. Zhang Z, Zwick S, Loew E, Grimley JS, Ramanathan S. Mouse embryo geometry drives formation of robust signaling gradients through receptor localization. Nat Commun. 2019; 10 doi: 10.1038/s41467-019-12533-7

[12]. Yamachika E, Tsujigiwa H, Shirasu N, Ueno T, Sakata Y, Fukunaga J, Mizukawa N, Yamada M, Sugahara T. Immobilized recombinant human bone morphogenetic protein-2 enhances the phosphorylation of receptor-activated Smads. J Biomed Mater Res - Part A. 2008; 88: 599–607. DOI: 10.1002/jbm.a.31833

[13]. Llopis-Hernández V, Cantini M, González-García C, Cheng ZA, Yang J, Tsimbouri PM, García AJ, Dalby MJ, Salmerón-Sánchez M. Material-driven fibronectin assembly for high-efficiency presentation of growth factors. Sci Adv. 2016; 2 e1600188 doi: 10.1126/sciadv.1600188 [PubMed: 27574702]

[14]. Crouzier T, Ren K, Nicolas C, Roy C, Picart C. Layer-by-layer films as a biomimetic reservoir for rhBMP-2 delivery: Controlled differentiation of myoblasts to osteoblasts. Small. 2009; 5: 598–608. DOI: 10.1002/smll.200800804 [PubMed: 19219837]

[15]. Gamell C, Osses N, Bartrons R, Rückle T, Camps M, Rosa JL, Ventura F. BMP2 induction of actin cytoskeleton reorganization and cell migration requires PI3-kinase and Cdc42 activity. J Cell Sci. 2008; 121: 3960–3970. DOI: 10.1242/jcs.031286 [PubMed: 19001503]

[16]. Khurana S, Buckley S, Schouteden S, Ekker S, Petryk A, Delforge M, Zwijsen A, Verfaillie CM. Anovel role of BMP4 in adult hematopoietic stem and progenitor cell homing via Smad independent regulation of integrin-α4 expression. Blood. 2013; 121: 781–790. DOI: 10.1182/blood-2012-07-446443 [PubMed: 23243277]

[17]. Migliorini E, Guevara-Garcia A, Albiges-Rizo C, Picart C. Learning from BMPs and their biophysical extracellular matrix microenvironment for biomaterial design. Bone. 2020; 141 115540 doi: 10.1016/j.bone.2020.115540 [PubMed: 32730925]

[18]. Morrell NW, Bloch DB, Ten Dijke P, Goumans MJTH, Hata A, Smith J, Yu PB, Bloch KD. Targeting BMP signalling in cardiovascular disease and anaemia. Nat Rev Cardiol. 2016; 13: 106–120. DOI: 10.1038/nrcardio.2015.156 [PubMed: 26461965]

[19]. Hynes RO. The extracellular matrix: Not just pretty fibrils. Science (80-). 2009; 326: 1216–1219. DOI: 10.1126/science.1176009

[20]. Tenney RM, Discher DE. Stem cells, microenvironment mechanics, and growth factor activation. Curr Opin Cell Biol. 2009; 21: 630–635. DOI: 10.1016/j.ceb.2009.06.003 [PubMed: 19615877]

[21]. Ashe HL. Modulation of BMP signalling by integrins. Biochem Soc Trans. 2016; 44: 1465–1473. DOI: 10.1042/BST20160111 [PubMed: 27911728]

[22]. Wei Q, Holle A, Li J, Posa F, Biagioni F, Croci O, Benk AS, Young J, Noureddine F, Deng J, Zhang M, et al. BMP-2 Signaling and Mechanotransduction Synergize to Drive Osteogenic Differentiation via YAP/TAZ. Adv Sci. 2020; 7: 1–15. DOI: 10.1002/advs.201902931

[23]. Crouzier T, Fourel L, Boudou T, Albigès-Rizo C, Picart C. Presentation of BMP-2 from a soft biopolymeric film unveils its activity on cell adhesion and migration. Adv Mater. 2011; 23: H111–H118. DOI: 10.1002/adma.201004637 [PubMed: 21433098]

[24]. Machillot P, Quintal C, Dalonneau F, Hermant L, Monnot P, Matthews K, Fitzpatrick V, Liu J, Pignot-Paintrand I, Picart C. Automated Buildup of Biomimetic Films in Cell Culture Microplates for High-Throughput Screening of Cellular Behaviors. Adv Mater. 2018; 30: 1–8. DOI: 10.1002/adma.201801097

[25]. Bouyer M, Guillot R, Lavaud J, Plettinx C, Olivier C, Curry V, Boutonnat J, Coll JL, Peyrin F, Josserand V, Bettega G, et al. Surface delivery of tunable doses of BMP-2 from an adaptable polymeric scaffold induces volumetric bone regeneration. Biomaterials. 2016; 104: 168–181. DOI: 10.1016/j.biomaterials.2016.06.001 [PubMed: 27454063]

[26]. Fourel L, Valat A, Faurobert E, Guillot R, Bourrin-Reynard I, Ren K, Lafanechère L, Planus E, Picart C, Albiges-Rizo C. β3 integrin-mediated spreading induced by matrix-bound BMP-2 controls Smad signaling in a stiffness-independent manner. J Cell Biol. 2016; 212: 693–706. DOI: 10.1083/jcb.201508018 [PubMed: 26953352]

[27]. Sefkow-Werner J, Machillot P, Sales A, Castro-Ramirez E, Degardin M, Boturyn D, Cavalcanti-Adam EA, Albiges-Rizo C, Picart C, Migliorini E. Heparan sulfate co-immobilized with cRGD ligands and BMP2 on biomimetic platforms promotes BMP2-mediated osteogenic differentiation. Acta Biomater. 2020; 114: 90–103. DOI: 10.1016/j.actbio.2020.07.015 [PubMed: 32673751]

[28]. Posa F, Baha-Schwab EH, Wei Q, Di Benedetto A, Neubauer S, Reichart F, Kessler H, Spatz JP, Albigez-Rizo C, Mori G, Cavalcanti-Adam EA. Surface Co-presentation of BMP-2 and integrin selective ligands at the nanoscale favors α5β1 integrin-mediated adhesion. Biomaterials. 2021; 267 120484 doi: 10.1016/j.biomaterials.2020.120484 [PubMed: 33142116]

[29]. Toofan P, Wheadon H. Role of the bone morphogenic protein pathway in developmental haemopoiesis and leukaemogenesis. Biochem Soc Trans. 2016; 44: 1455–1463. DOI: 10.1042/BST20160104 [PubMed: 27911727]

[30]. Sovershaev TA, Unruh D, Sveinbjørnsson B, Fallon JT, Hansen JB, Bogdanov VY, Sovershaev MA. A novel role of bone morphogenetic protein-7 in the regulation of adhesion and migration of human monocytic cells. Thromb Res. 2016; 147: 24–31. DOI: 10.1016/j.thromres.2016.09.018 [PubMed: 27669124]

[31]. Fujioka-Kobayashi M, Sawada K, Kobayashi E, Schaller B, Zhang Y, Miron RJ. Osteogenic potential of rhBMP9 combined with a bovine-derived natural bone mineral scaffold compared to rhBMP2. Clin Oral Implants Res. 2017; 28: 381–387. DOI: 10.1111/clr.12804 [PubMed: 26988608]

[32]. Ye L, Kynaston H, Jiang WG. Bone morphogenetic protein-9 induces apoptosis in prostate cancer cells, the role of prostate apoptosis response-4. Mol Cancer Res. 2008; 6: 1594–1606. DOI: 10.1158/1541-7786.MCR-08-0171 [PubMed: 18922975]

[33]. Rivera JC, Strohbach CA, Wenke JC, Rathbone CR. Beyond osteogenesis: An in vitro comparison of the potentials of six bone morphogenetic proteins. Front Pharmacol. 2013; 4: 1–7. DOI: 10.3389/fphar.2013.00125 [PubMed: 23346057]

[34]. Gilde F, Fourel L, Guillot R, Pignot-Paintrand I, Okada T, Fitzpatrick V, Boudou T, Albiges-Rizo C, Picart C. Stiffness-dependent cellular internalization of matrix-bound BMP-2 and its relation to Smad and non-Smad signaling. Acta Biomater. 2016; 46: 55–67. DOI: 10.1016/j.actbio.2016.09.014 [PubMed: 27633320]

[35]. Roberts SJ, Chen Y, Moesen M, Schrooten J, Luyten FP. Enhancement of osteogenic gene expression for the differentiation of human periosteal derived cells. Stem Cell Res. 2011; 7: 137–144. DOI: 10.1016/j.scr.2011.04.003 [PubMed: 21763621]

[36]. Duchamp De Lageneste O, Julien A, Abou-Khalil R, Frangi G, Carvalho C, Cagnard N, Cordier C, Conway SJ, Colnot C. Periosteum contains skeletal stem cells with high bone regenerative potential controlled by Periostin. Nat Commun. 2018; 9: 1–15. DOI: 10.1038/s41467-018-03124-z [PubMed: 29317637]

[37]. Bolander J, Ji W, Geris L, Bloemen V, Chai YC, Schrooten J, Luyten FP. The combined mechanism of bone morphogenetic protein- and calcium phosphate-induced skeletal tissue formation by human periosteum derived cells. Eur Cells Mater. 2016; 31: 11–25. DOI: 10.22203/eCM.v031a02

[38]. Schneider A, Francius G, Obeid R, Schwinté P, Hemmerlé J, Frisch B, Schaaf P, Voegel JC, Senger B, Picart C. Polyelectrolyte multilayers with a tunable young's modulus: Influence of film stiffness on cell adhesion. Langmuir. 2006; 22: 1193–1200. DOI: 10.1021/la0521802 [PubMed: 16430283]

[39]. Crouzier T, Sailhan F, Becquart P, Guillot R, Logeart-Avramoglou D, Picart C. The performance of BMP-2 loaded TCP/HAP porous ceramics with a polyelectrolyte multilayer film coating. Biomaterials. 2011; 32: 7543–7554. DOI: 10.1016/j.biomaterials.2011.06.062 [PubMed: 21783243]

[40]. Crouzier T, Ren K, Nicolas C, Roy C, Picart C. Layer-By-Layer Films as a Biomimetic Reservoir for rhBMP-2 Delivery : Controlled Differentiation of Myoblasts to Osteoblasts. Small. 2009; 598–608. DOI: 10.1002/smll.200800804 [PubMed: 19219837]

[41]. Bidart M, Ricard N, Levet S, Samson M, Mallet C, David L, Subileau M, Tillet E, Feige JJ, Bailly S. BMP9 is produced by hepatocytes and circulates mainly in an active mature form complexed to its prodomain. Cell Mol Life Sci. 2012; 69: 313–324. DOI: 10.1007/s00018-011-0751-1 [PubMed: 21710321]

[42]. Sieber C, Kopf J, Hiepen C, Knaus P. Recent advances in BMP receptor signaling. Cytokine Growth Factor Rev. 2009; 20: 343–355. DOI: 10.1016/j.cytogfr.2009.10.007 [PubMed: 19897402]

[43]. Yadin D, Knaus P, Mueller TD. Structural insights into BMP receptors: Specificity, activation and inhibition. Cytokine Growth Factor Rev. 2016; 27: 13–34. DOI: 10.1016/j.cytogfr.2015.11.005 [PubMed: 26690041]

[44]. Holtzhausen A, Golzio C, How T, Lee YH, Schiemann WP, Katsanis N, Blobe GC. Novel bone morphogenetic protein signaling through Smad2 and Smad3 to regulate cancer progression and development. FASEB J. 2014; 28: 1248–1267. DOI: 10.1096/fj.13-239178 [PubMed: 24308972]

[45]. Eyckmans J, Lin GL, Chen CS. Adhesive and mechanical regulation of mesenchymal stem cell differentiation in human bone marrow and periosteum-derived progenitor cells. Biol Open. 2012; 1: 1158–1168. DOI: 10.1242/bio.20122162

[46]. Valia Khodr CP, Machillot Paul, Migliorini Elisa, Reiser Jean-Baptiste. High throughput measurements of BMP/BMP receptors interactions using bio-layer interferometry. BioRxiv. 2020; doi: 10.1101/2020.10.20.348060

[47]. Huang RL, Sun Y, Ho CK, Liu K, Tang QQ, Xie Y, Li Q. IL-6 potentiates BMP-2-induced osteogenesis and adipogenesis via two different BMPR1A-mediated pathways article. Cell Death Dis. 2018; 9 doi: 10.1038/s41419-017-0126-0

[48]. Khurana S, Melacarne A, Yadak R, Schouteden S, Notelaers T, Pistoni M, Maes C, Verfaillie CM. SMAD signaling regulates CXCL12 expression in the bone marrow niche, affecting homing and mobilization of hematopoietic progenitors. Stem Cells. 2014; 32: 3012–3022. DOI: 10.1002/stem.1794 [PubMed: 25069965]

[49]. Haupt J, Stanley A, McLeod CM, Cosgrove BD, Culbert AL, Wang L, Mourkioti F, Mauck RL, Shore EM. ACVR1 R206H FOP mutation alters mechanosensing and tissue stiffness during heterotopic ossification. Mol Biol Cell. 2019; 30: 17–29. DOI: 10.1091/mbc.E18-05-0311 [PubMed: 30379592]

[50]. Peart TM, Correa RJM, Valdes YR, DiMattia GE, Shepherd TG. BMP signalling controls the malignant potential of ascites-derived human epithelial ovarian cancer spheroids via AKT kinase activation. Clin Exp Metastasis. 2012; 29: 293–313. DOI: 10.1007/s10585-011-9451-3 [PubMed: 22249415]

[51]. Derynck R, Budi EH. Specificity, versatility, and control of TGF-b family signaling. Sci Signal. 2019; 12 doi: 10.1126/scisignal.aav5183

[52]. Piek E, Moustakas A, Kurisaki A, Heldin CH, Ten Dijke P. TGF-β type I receptor/ALK-5 and Smad proteins mediate epithelial to mesenchymal transdifferentiation in NMuMG breast epithelial cells. J Cell Sci. 1999; 112: 4557–4568. [PubMed: 10574705]

[53]. Egorova AD, Khedoe PPSJ, Goumans MJTH, Yoder BK, Nauli SM, Ten Dijke P, Poelmann RE, Hierck BP. Lack of primary cilia primes shear-induced endothelial-to-mesenchymal transition. Circ Res. 2011; 108: 1093–1101. DOI: 10.1161/CIRCRESAHA.110.231860 [PubMed: 21393577]

[54]. Walshe TE, Dela Paz NG, D'Amore PA. The role of shear-induced transforming growth factor-β signaling in the endothelium. Arterioscler Thromb Vasc Biol. 2013; 33: 2608–2617. DOI: 10.1161/ATVBAHA.113.302161 [PubMed: 23968981]

[55]. Sanz-Ramos P, Dotor J, Izal-Azcárate I. The role of Alk-1 and Alk-5 in the mechanosensing of chondrocytes. Cell Mol Biol Lett. 2014; 19: 659–674. DOI: 10.2478/s11658-014-0220-6 [PubMed: 25424912]

[56]. Ding Q, Subramanian I, Luckhardt TR, Che P, Waghray M, Zhao XK, Bone N, Kurundkar AR, Hecker L, Hu M, Zhou Y, et al. Focal adhesion kinase signaling determines the fate of lung epithelial cells in response to TGF-β. Am J Physiol - Lung Cell Mol Physiol. 2017; 312: L926–L935. DOI: 10.1152/ajplung.00121.2016 [PubMed: 28360109]

[57]. Matos AM, Gonçalves AI, Rodrigues MT, Miranda MS, Haj AJE, Reis RL, Gomes ME. Remote triggering of TGF-β/Smad2/3 signaling in human adipose stem cells laden on magnetic scaffolds synergistically promotes tenogenic commitment. Acta Biomater. 2020; 113: 488–500. DOI: 10.1016/j.actbio.2020.07.009 [PubMed: 32652226]

[58]. Schiller HB, Hermann MR, Polleux J, Vignaud T, Zanivan S, Friedel CC, Sun Z, Raducanu A, Gottschalk KE, Théry M, Mann M, et al. β 1 - And α v-class integrins cooperate to regulate myosin II during rigidity sensing of fibronectin-based microenvironments. Nat Cell Biol. 2013; 15: 625–636. DOI: 10.1038/ncb2747 [PubMed: 23708002]

[59]. Brunner M, Millon-Frémillon A, Chevalier G, Nakchbandi IA, Mosher D, Block MR, Albigès-Rizo C, Bouvard D. Osteoblast mineralization requires β1 integrin/ICAP-1-dependent fibronectin deposition. J Cell Biol. 2011; 194: 307–322. DOI: 10.1083/jcb.201007108 [PubMed: 21768292]

[60]. Moursi, A, Globus, R. C.D.-J. of cell Science, U. 1997, Interactions between integrin receptors and fibronectin are required for.pdf. Vol. 2196. JcsBiologistsOrg; 1997. 2187–2196. http://jcs.biologists.org/content/110/18/2187.short

[61]. Wang W, Kirsch T. Annexin V/β5 integrin interactions regulate apoptosis of growth plate chondrocytes. J Biol Chem. 2006; 281: 30848–30856. DOI: 10.1074/jbc.M605937200 [PubMed: 16914549]

[62]. Hamidouche Z, Fromigué O, Ringe J, Häupl T, Vaudin P, Pagès JC, Srouji S, Livne E, Marie PJ. Priming integrin α5 promotes human mesenchymal stromal cell osteoblast differentiation and osteogenesis. Proc Natl Acad Sci U S A. 2009; 106: 18587–18591. DOI: 10.1073/pnas.0812334106 [PubMed: 19843692]

[63]. Lai CF, Bai S, Uthgenannt BA, Halstead LR, McLoughlin P, Schafer BW, Chu PH, Chen J, Otey CA, Cao X, Cheng SL. Four and Half Lim Protein 2 (FHL2) stimulates osteoblast differentiation. J Bone Miner Res. 2006; 21: 17–28. DOI: 10.1359/JBMR.050915 [PubMed: 16355270]

[64]. Zhao HJ, Klausen C, Li Y, Zhu H, Wang YL, Leung PCK. Bone morphogenetic protein 2 promotes human trophoblast cell invasion by upregulating N-cadherin via non-canonical SMAD2/3 signaling. Cell Death Dis. 2018; 9: 4–15. DOI: 10.1038/s41419-017-0230-1 [PubMed: 29305580]

[65]. Upton PD, Davies RJ, Tajsic T, Morrell NW. Transforming growth factor-β1 represses bone morphogenetic protein-mediated Smad signaling in pulmonary artery smooth muscle cells via Smad3. Am J Respir Cell Mol Biol. 2013; 49: 1135–1145. DOI: 10.1165/rcmb.2012-0470OC [PubMed: 23937428]

[66]. Klatte-Schulz F, Giese G, Differ C, Minkwitz S, Ruschke K, Puts R, Knaus P, Wildemann B. An investigation of BMP-7 mediated alterations to BMP signalling components in human tenocyte-like cells. Sci Rep. 2016; 6: 1–11. DOI: 10.1038/srep29703 [PubMed: 28442746]

[67]. Perron JC, Rodrigues AA, Surubholta N, Dodd J. Chemotropic signaling by BMP7 requires selective interaction at a key residue in ActRIIA. Biol Open. 2019; 8 doi: 10.1242/bio.042283

[68]. Finnson KW, Almadani Y, Philip A. Non-canonical (non-SMAD2/3) TGF-β signaling in fibrosis: Mechanisms and targets. Semin Cell Dev Biol. 2020; 101: 115–122. DOI: 10.1016/j.semcdb.2019.11.013 [PubMed: 31883994]

[69]. Rosen V. BMP and BMP inhibitors in bone. Ann N Y Acad Sci. 2006; 1068: 19–25. DOI: 10.1196/annals.1346.005 [PubMed: 16831902]

[70]. Ohte S, Shin M, Sasanuma H, Yoneyama K, Akita M, Ikebuchi K, Jimi E, Maruki Y, Matsuoka M, Namba A, Tomoda H, et al. A novel mutation of ALK2, L196P, found in the most benign case of fibrodysplasia ossificans progressiva activates BMP-specific intracellular signaling equivalent to a typical mutation, R206H. Biochem Biophys Res Commun. 2011; 407: 213–218. DOI: 10.1016/j.bbrc.2011.03.001 [PubMed: 21377447]

[71]. Aoki H, Fujii M, Imamura T, Yagi K, Takehara K, Kato M, Miyazono K. Synergistic effects of different bone morphogenetic protein type I receptors on alkaline phosphatase induction. J Cell Sci. 2001; 114: 1483–1489. [PubMed: 11282024]

[72]. Goh BC, Singhal V, Herrera AJ, Tomlinson RE, Kim S, Faugere MC, Germain-Lee EL, Clemens TL, Lee SJ, Digirolamo DJ. Activin receptor type 2A (ACVR2A) functions directly in osteoblasts as a negative regulator of bone mass. J Biol Chem. 2017; 292: 13809–13822. DOI: 10.1074/jbc.M117.782128 [PubMed: 28659341]

Europe PMC Funders Author Manuscripts

Europe PMC Funders Author Manuscripts

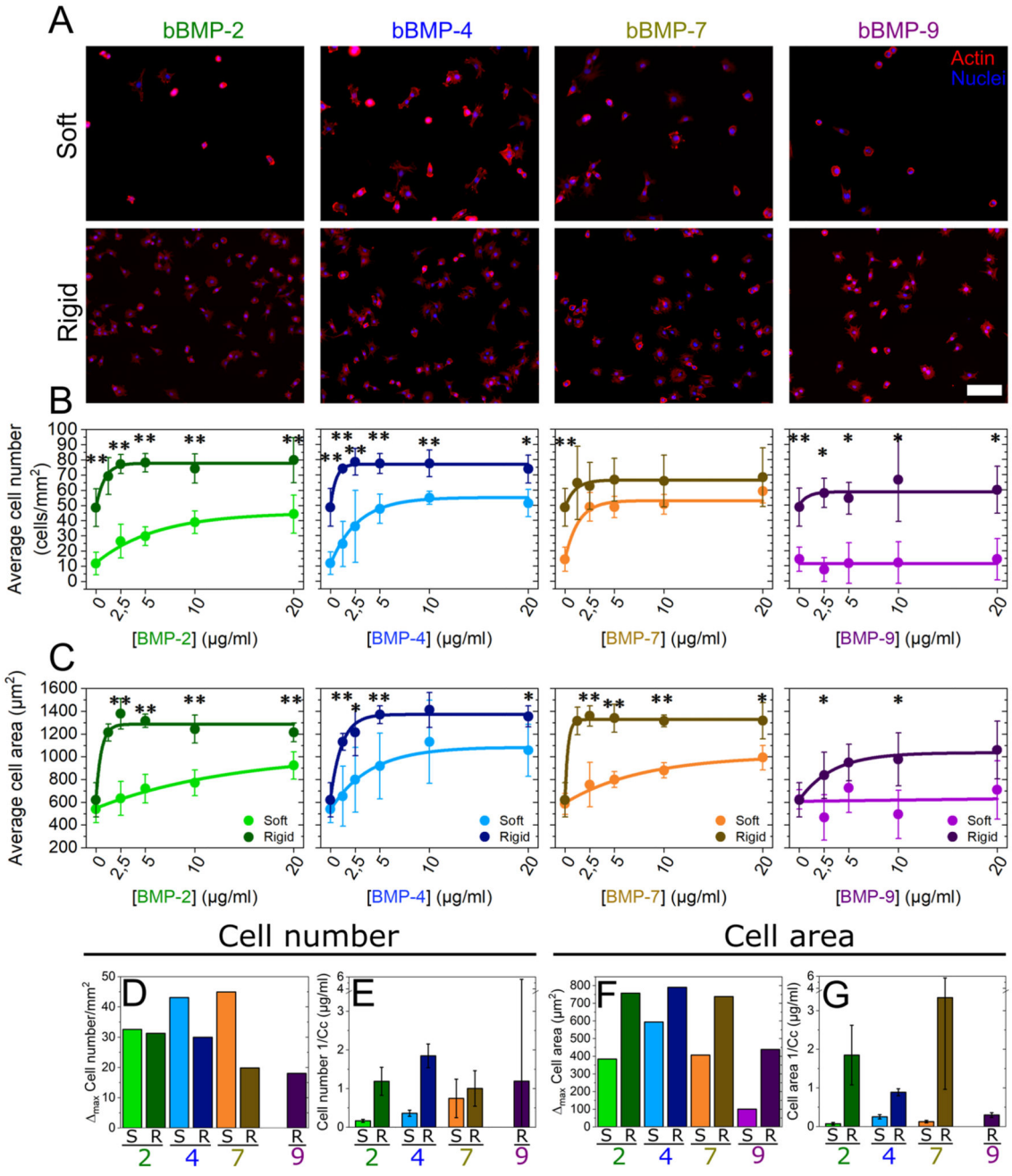

Fig. 1. Quantification of C2C12 cell adhesion and spreading on soft and rigid films with four bBMPs (2, 4, 7, 9) at increasing BMP-loading concentrations.

Representative fluorescent images of the actin cytoskeleton for (**a**) cells cultured for 5 h on soft films (S) and for 4 h on rigid films (R). Images correspond to a BMP loading concentration in solution of 5 μg/mL. Quantification of (**b**) the average cell number per mm^2 of substrate area and (**c**) the cell area as a function of the initial BMP concentration in the loading solution. Results of the data fitting for each BMP-dose response curve (see methods) gave two parameters: Δ_{max} and Cc (characteristic concentration). (**d**) Difference

(Δ_{max}) between the maximum cell number and the no bBMP condition, plotted for each of the 4 bBMPs and film stiffness (S, R films). (**e**) Sensitivity to the BMP concentration (given as 1/Cc that provides a direct information on the sensitivity to the bBMP concentration). (**f** and **g**) Same quantitative parameters extracted for the cell spreading area in response to the bBMP-dose. Data represent three independent biological replicates with two microwells per condition in each independent experiment (technical replicates). Statistical tests were done using non-parametric Kruskal-Wallis ANOVA test to compare S (light color) and R (dark color) films (*$p < 0.05$; **$p < 0.01$). Scale bar=100 μm.

Europe PMC Funders Author Manuscripts

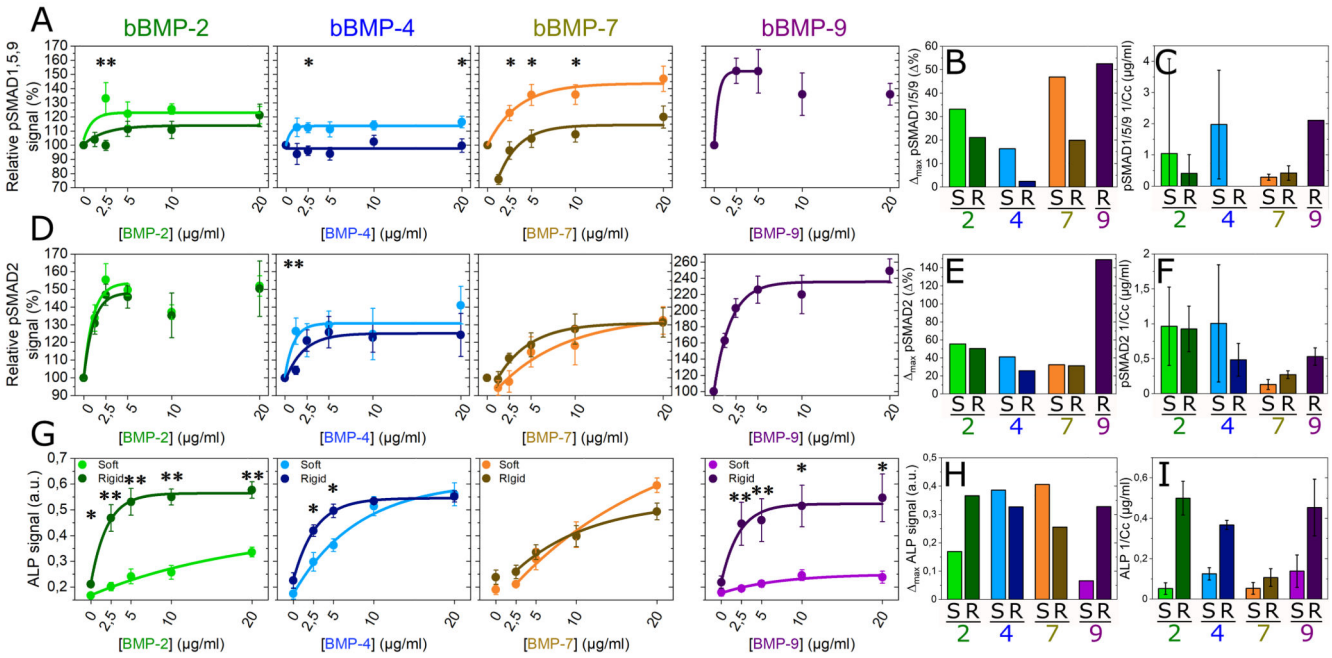

Fig. 2. pSMAD and ALP analyses for the four bBMPs on soft and rigid films.

Fluorescent signal quantification of (**a**) pSMAD1,5,9, (**d**) pSMAD2, and (**g**) ALP activity as a function of the BMP concentration in soft (S) (light color) and rigid (R) films (dark color). Quantitative parameters Δ_{max} and 1/Cc extracted from the fit of each of the experimental curves for (**b, c**) pSMAD1,5,9, (**e, f**) pSMAD2 and (**h, i**) ALP. Data represent the mean + SEM of 2 to 4 independent experiments with two samples per condition in each independent experiment (at least 400 cells were analyzed in total). Statistical tests were done using non-parametric Kruskal-Wallis ANOVA test to compare S and R films (*$p < 0.05$; **$p < 0.01$).

Europe PMC Funders Author Manuscripts

Europe PMC Funders Author Manuscripts

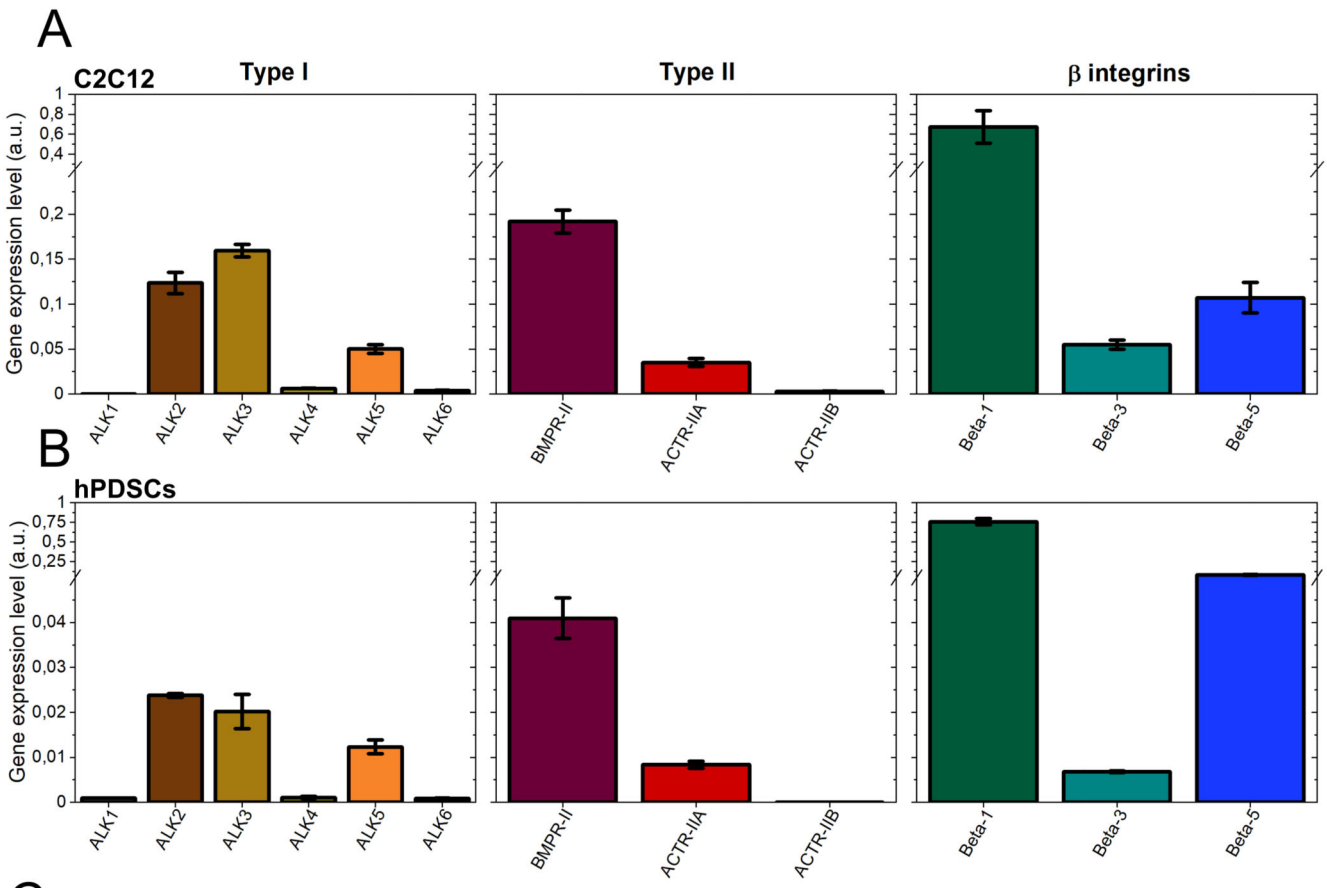

C

BMPR / BMP	Type I: ALK1 (AcvRL1)	Type I: ALK2 (AcvR1)	Type I: ALK3 (BMPR1a)	Type I: ALK5 (TGF-βR1)	Type I: ALK6 (BMPR1b)	Type II: BMPR-II	Type II: ACTR-IIA	Type II: ACTR-IIB
BMP-2	13 ± 1.6	7.0 ± 2.3	0.21 ± 0.03	5.8 ± 1.1	0.5 ± 0.1	5.4 ± 0.8	6.1 ± 1.2	6.3 ± 3.4
BMP-4	55.4 ± 4.0	10.5 ± 3.8	1.7 ± 0.5	21.9 ± 6.6	3.1 ± 0.3	56.0 ± 6.0	21.4 ± 3.7	26.0 ± 0.5
BMP-7	23.1 ± 2.1	18.4 ± 3.8	19.0 ± 2.1	22.6 ± 1.1	15.0 ± 1.2	5.5 ± 1.2	1.3 ± 0.3	7.1 ± 0.7
BMP-9	0.2 ± 0.1	133.1 ± 35.1	N.A	51.0 ± 18.3	N.A	0.8 ± 0.2	1.7 ± 0.1	1.4 ± 0.4

Fig. 3. Differentiation of hPDSCs in the osteogenic, chondrogenic or adipogenic pathways analyzed using qPCR of relevant markers.

Relative gene expression was analyzed for hPDSCs cultured for three days on the soft (S) and rigid (R) films with bBMPs using qPCR for (**a-c**) osteogenic markers: osterix, DLX5, osteopontin, (**d-f**) chondrogenic markers: Sox9, aggrecan, Col2A1, and (**g-i**) adipogenic markers: PPARγ, C/Ebp a and adiponectin. Expression of each gene was normalized to the expression of three reference genes: EF1, PPIA and GUSB. In order to compare the experimental conditions, all gene expression values were then re-normalized to the “soft film with no BMP condition”, which was set to 1. Data are represented as mean + SEM of three independent experiments. Statistical tests were done using non-parametric Kruskal-Wallis ANOVA test to compare S and R films (*$p < 0.05$; **$p < 0.01$).

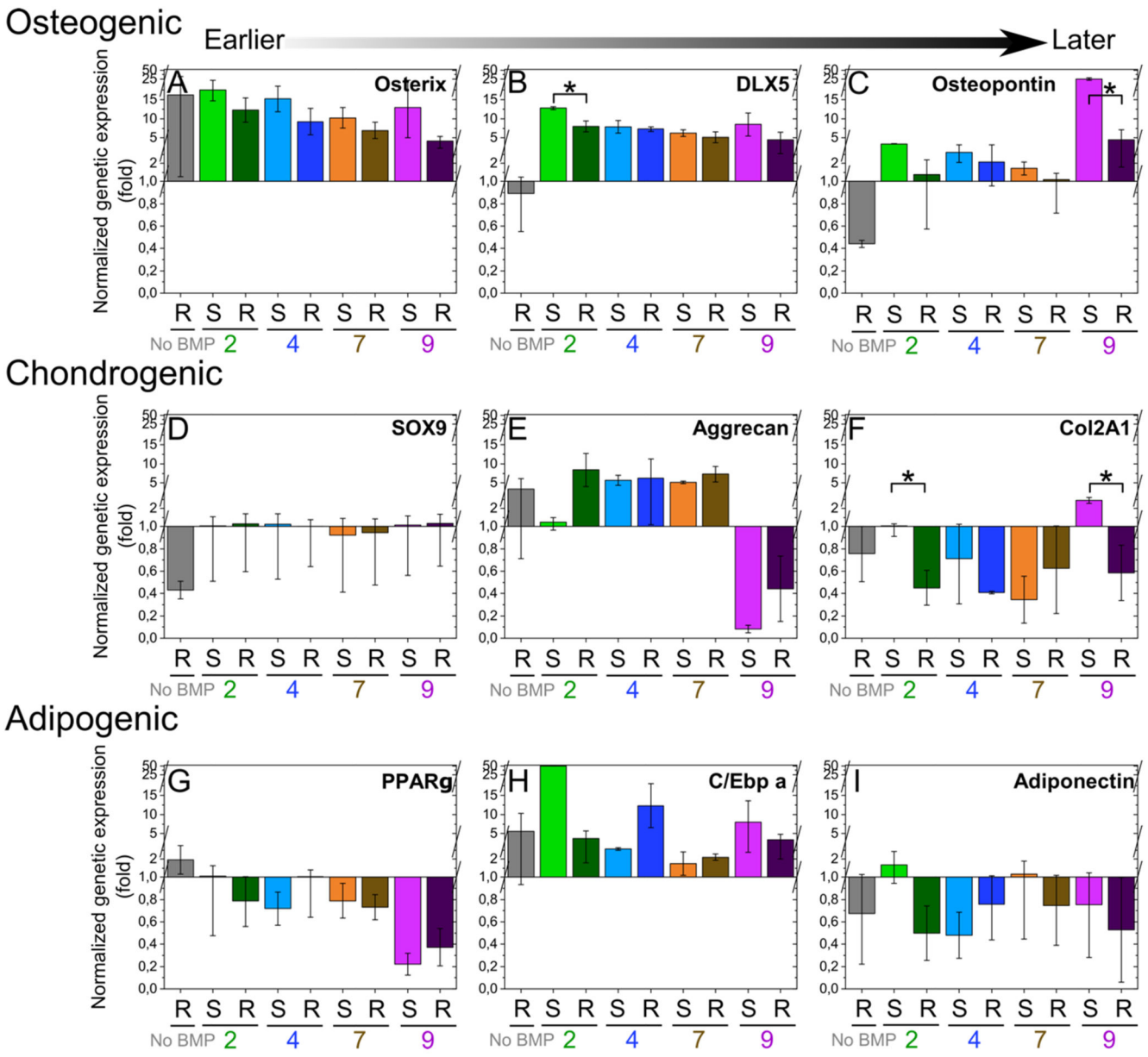

Fig. 4. Relative gene expression analysis of type I, type II BMP receptors and β-integrins.

Data corresponding to (**a**) C2C12 cells and to (**b**) hPDSCs. The gene expression was analyzed by qPCR and it was normalized to the expression of EF1, PPIA and GUSB genes. Data are represented as mean + SEM of three independent experiments. (**c**) Table of the affinity constants (Kd in nM) of the type I and II BMP receptors with the four selected BMPs. Data was obtained from kinetic experiments performed by bio-layer interferometry (BLI), from the work of Khodr *et al.* [46]. The highest affinity couples (Kd < 5 nM) are highlighted in dark blue, those with an affinity in the range from 5 to 25 nM are in light blue. N.A means no measurable interaction. Values are given as mean ± SD of three independent experiments.

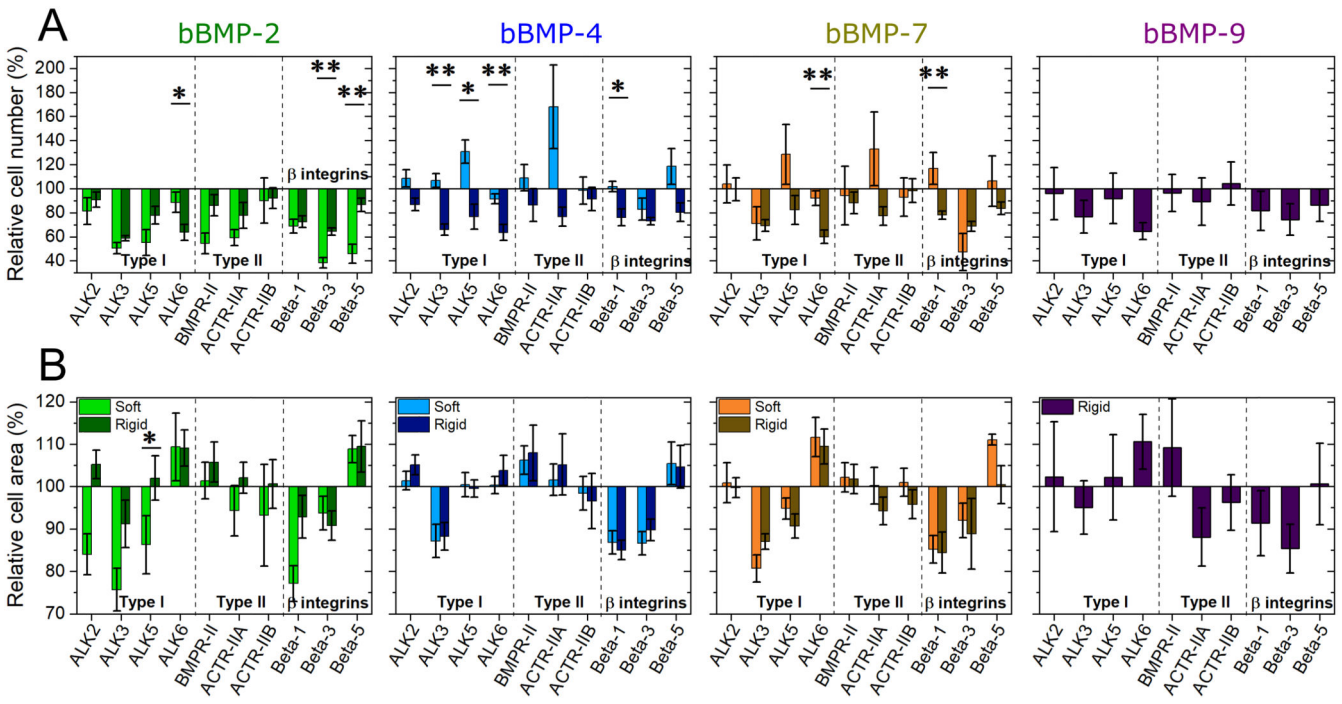

Fig. 5. Effect of BMP receptor and β chain integrin silencing on cell adhesion and spreading.

C2C12 cells were transfected with siRNA against BMP receptor type I (ALK2, ALK3, ALK5, ALK6), BMP receptor type II (BMPR-II, ACTR-IIA, ACTR-IIB) and β chain integrins (β1, β3, β5) and plated on soft (light color) and rigid (dark color) films with bBMPs for 5 or 4 h, respectively. The cell number par mm^2 of substrate area and the spreading area were quantified. The relative % is given, in comparison to a control scrambled siRNA. (**a**) Relative cell number (%), (**b**) relative cell area (%). Data represent the mean ± SEM, with 3 biological replicates and 2 technical replicates per experiment. Statistical tests were done using non-parametric Kruskal-Wallis ANOVA test (*, $p \leq 0.05$; **, $p \leq 0.01$). Statistical comparisons were made between soft and rigid films for each condition.

Europe PMC Funders Author Manuscripts

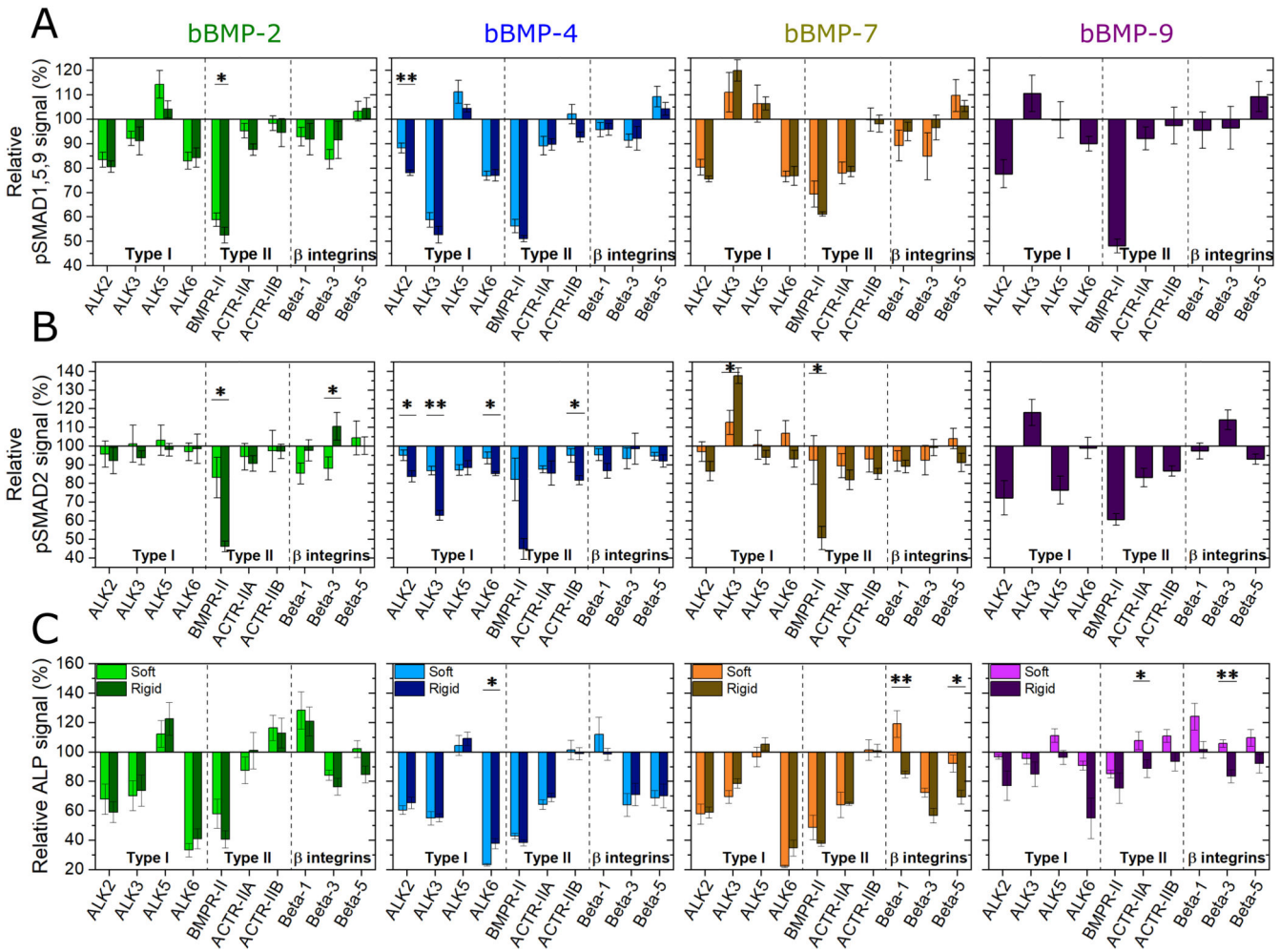

Fig. 6. Effect of BMP receptor and β chain integrin silencing on early cell differentiation to bone.

C2C12 cells were transfected with siRNA against BMP receptor type I (ALK2, ALK3, ALK5, ALK6), BMP receptor type II (BMPR-II, ACTR-IIA, ACTR-IIB) and β chain integrins (β1, β3, β5) and plated on soft (light color) and rigid (dark color) films with bBMPs for 5 or 4 h, respectively. (**a**) pSMAD1,5,9 signal and (**b**) ALP activity were quantified, and the relative % is given, in comparison to a control scrambled siRNA. Data represent the mean ± SEM. Statistical tests were done using non-parametric Kruskal-Wallis ANOVA test (*, $p \leq 0.05$; **, $p \leq 0.01$). Statistical comparisons were made between soft and rigid films for each condition.

Europe PMC Funders Author Manuscripts

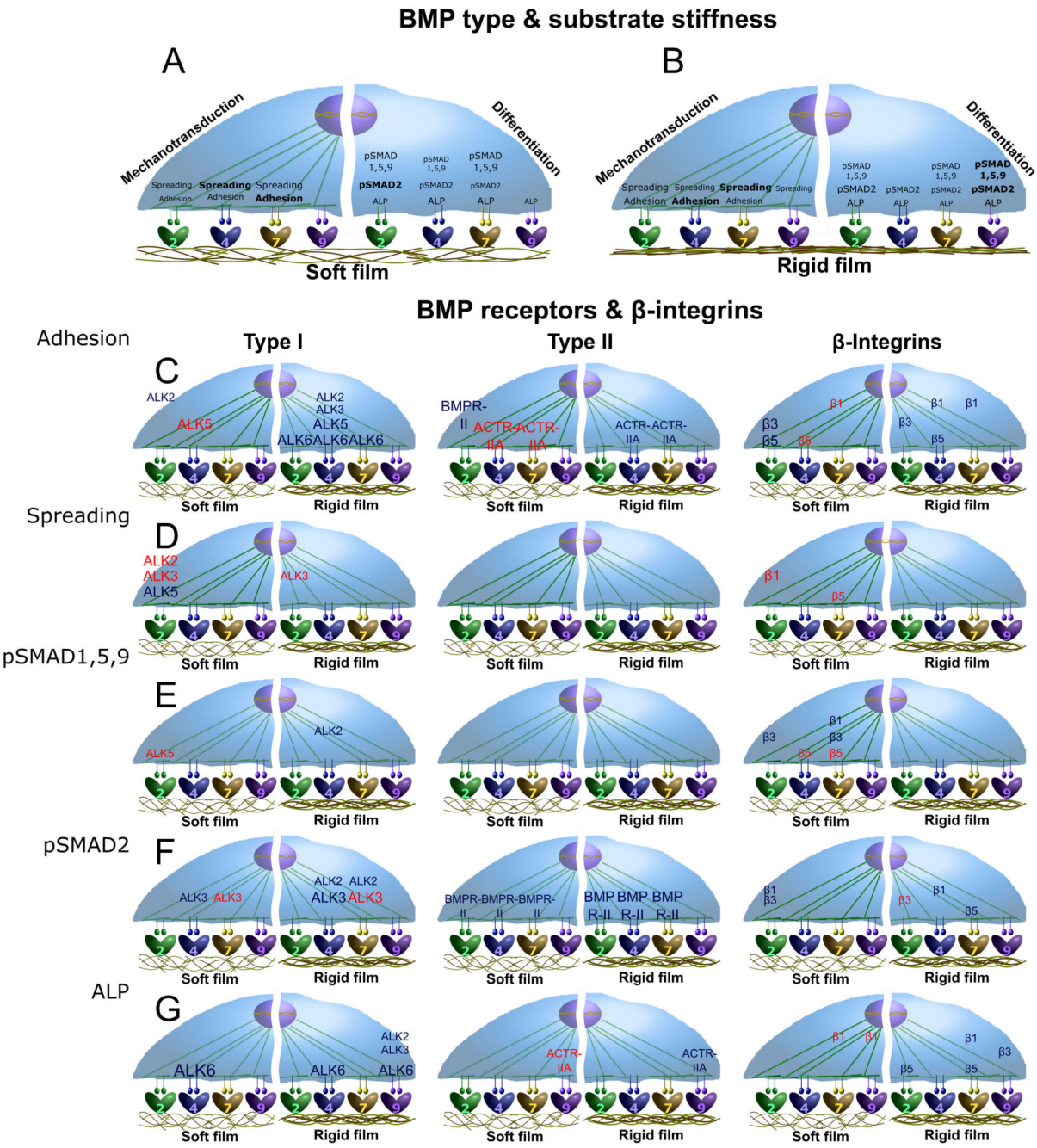

Fig. 7. Schematic representations summarizing the major results of this study.

The influence of the four bBMPs on C2C12 cell adhesion and spreading, as mechanotransduction parameters, and pSMAD1,5,9, pSMAD2 and ALP activity, as differentiation parameters, is represented for (**a**) soft and (**b**) rigid films. Moreover, the role of the BMP receptors type I, type II and the three β chain integrins analyzed, on the mechanotransduction and differentiation parameters aforementioned, are depicted for each type of receptor: (**c**) type I BMPR, (**d**) type II BMPR, and (**e**) β chain integrins. Since

no relevant stiffness-dependent differences were generally observed for the receptors, no specific detailed distinction between soft and rigid films is represented.

Europe PMC Funders Author Manuscripts

Table 1

Table summarizing the role of BMP receptors and of integrins in cell adhesion and bone differentiation as assessed using siRNA of the targetted receptors (Figure 5 and 6, figure SI 14 and 16). For each studied parameters, the role of the type I, type II BMPR and of integrins is indicated. The receptors are classified as stiffness-independent or stiffness-dependent. “R” is the rigid condition, and “S” is the soft condition. “+” symbol represents an activator role (< 100%), and “-”an inhibitory role (> 100%) of the receptor.

Role of BMPR and integrins in	Stiffness-independent	Stiffness-dependent
Cell adhesion	**ALK3** (+ bBMP-2/7/9) **ALK5** (++ bBMP-2) **ACTR-IIA** (++ bBMP-2) **Beta1**(+ bBMP-2) **Beta3** (+ bBMP-4; ++ bBMP-7)	**ALK2** (+ for bBMP-2, +/- for bBMP-4) **ALK3** (**R**+ bBMP-4) **ALK5** (**S** --, **R** ++ bBMP-4) **ALK6 (R** ++ bBMP-2/4/7) **BMPR-II** (**S** ++ bBMP-2) **ACTR-IIA** (**S** --, **R** + bBMP-4/7) **Beta1** (**R** + bBMP-4; **S** -, **R** + bBMP-7) **Beta3** (**S ++, R** + bBMP-2) **Beta5** (**S** ++ bBMP-2; **S** -, **R** + bBMP-4)
Cell spreading	**ALK3** (++ bBMP-4/7) **ALK6** (- bBMP-2/7) **Beta1** (++ bBMP-4/7/9) **Beta3** (+ bBMP-2/4/7/9) **Beta5** (-bBMP-2/4)	**ALK2** (**S** -- bBMP-2) **ALK3** (**S** --, **R**- bBMP-2) **ALK5** (**S** ++ bBMP-2) **Beta1** (**S** -- bBMP-2) **Beta5** (**S** - bBMP-7)
SMAD 1,5,9 signaling	**ALK2** (+ bBMP-2/7/9) **ALK3** (++ bBMP-4; -- bBMP-7/9) **ALK6** (+ BMP-2/4/7/9) **Beta1** (+ bBMP-2) **Beta3** (+ bBMP-4)	**ALK2** (**R**+ bBMP-4) **ALK5** (**S** - bBMP-2) **Beta1** (**S** + bBMP-7) **Beta3** (**S** + bBMP-2/7) **Beta5** (**S** - bBMP-4/7)
SMAD 2 signaling	**ALK2** (++ bBMP-9) **ALK5** (+ bBMP-4; ++ bBMP-9) **BMPR-II** (++ bBMP-9)	**ALK2** (**R** + bBMP-4/7) **ALK3** (**S** +, **R** ++ bBMP-4; **S** -, **R** -- bBMP-7) Role of BMPR-II even w/o BMP **BMPR-II** (**S** +, **R** ++ bBMP-2/4/7) **Beta1** (**S** + bBMP-2; **R** + bBMP-4) **Beta3** (**S** +, **R** - bBMP-2) **Beta5** (**R** + bBMP-7)
ALP	**ALK2** (+ BMP-2/4/7) **ALK3** (+ for BMP-2/4/7) **ALK6** (++ bBMP-2/7) **BMPR-II** (++ bBMP-2/4/7; + bBMP-9) **ACTRIIA** (+ bBMP-4/7) **Beta1** (- bBMP-2) **Beta3** (+ bBMP-2/4/7) **Beta5** (+ bBMP-4)	**ALK2**(**R** + bBMP-9) **ALK3** (**R** + bBMP-9) **ALK6** (**S** +++, **R** ++ bBMP-4; **R** ++bBMP-9) **ACTRIIA** (**S**-, **R** + bBMP-9) **Beta1** (**S**-, R + bBMP-7; **S**- bBMP-9) **Beta3** (**R** + bBMP-9) **Beta5** (**R** + bBMP-2/7)